Acta Oceanol. Sin., 2021, Vol. 40, No. 8, P. 14–31
https://doi.org/10.1007/s13131-021-1794-2
http://www.aosocean.com
E-mail: ocean2@hyxb.org.cn

Analysis of the spatial and temporal distributions of ecological variables and the nutrient budget in the Beibu Gulf

Huanglei Pan[1, 2], Dishi Liu[1, 3], Dalin Shi[1, 2], Shengyun Yang[1, 3], Weiran Pan[1, 3*]

[1] State Key Laboratory of Marine Environmental Science (Xiamen University), Xiamen 361102, China

[2] College of the Environment and Ecology, Xiamen University, Xiamen 361102, China

[3] College of Ocean and Earth Sciences, Xiamen University, Xiamen 361102, China

Received 31 May 2020; accepted 25 September 2020

Abstract

Based on a hydrodynamic-ecological model, the temperature, salinity, current, phytoplankton (Chl *a*), zooplankton, and nutrient (dissolved inorganic nitrogen, DIN, and dissolved inorganic phosphorous, DIP) distributions in the Beibu Gulf were simulated and the nutrient budget of 2015 was quantitatively analyzed. The simulated results show that interface processes and monsoons significantly influence the ecological processes in the gulf. The concentrations of DIN, DIP, phytoplankton and zooplankton are generally higher in the eastern and northern gulf than that in the western and southern gulf. The key regions affected by ecological processes are the Qiongzhou Strait in winter and autumn and the estuaries along the Guangxi coast and the Red River in summer. In most of the studied domains, biochemical processes contribute more to the nutrient budget than do physical processes, and the DIN and DIP increase over the year. Phytoplankton plays an important role in the nutrient budget; phytoplankton photosynthetic uptake is the nutrient sink, phytoplankton dead cellular release is the largest source of DIN, and phytoplankton respiration is the largest source of DIP. The nutrient flux in the connected sections of the Beibu Gulf and open South China Sea (SCS) inflows from the east and outflows to the south. There are 113 709 t of DIN and 5 277 t of DIP imported from the open SCS to the gulf year-around.

Key words: Beibu Gulf, hydrodynamic-ecological model, marine ecosystem, nutrient budget

Citation: Pan Huanglei, Liu Dishi, Shi Dalin, Yang Shengyun, Pan Weiran. 2021. Analysis of the spatial and temporal distributions of ecological variables and the nutrient budget in the Beibu Gulf. Acta Oceanologica Sinica, 40(8): 14–31, doi: 10.1007/s13131-021-1794-2

1 Introduction

The Beibu Gulf (16°00′–21°30′N, 105°40′–111°00′E) is an important semienclosed gulf located in the northwestern South China Sea (SCS) and is rich in natural resources (e.g., fish, oil, and tourist destinations); thus, it has considerable ecological and economical value (Han, 2013; Lin et al., 2008). The Beibu Gulf connects to the open SCS by the Qiongzhou Strait in the northeastern part and the open sea in the southern part (Fig. 1). It has a shallow depth of less than 100 m and has an area of approximately 12.8×10^4 km^2 (Chen et al., 2009a; Gao et al., 2013, 2017; Huang et al., 2008). The Red River in Vietnam and the Fangcheng River, Nanliu River, Qin River, Dafeng River, Beilun River, and Changhua River in China provide the major river discharges into the gulf, along with some smaller rivers along the coast (Chen et al., 2009a; Tang et al., 2003). The hydrological features and the general circulation in the gulf have strong seasonality, which are mainly driven by prevailing northeasterly monsoons from September to April and southwesterly monsoons during May to August; thus, the dynamic and biological processes are active (Chen et al., 2011; Gao et al., 2017; Huang et al., 2008; Tang et al., 2003).

Although the general environmental conditions in the Beibu Gulf are good, the fast development along the Beibu Gulf Economical Rim has placed the environment in the Beibu Gulf under pressure. According to marine environmental reports (Department of Ocean and Fisheries of Guangxi Zhuang Autonomous Region of China, 2013, 2016, 2017), some local areas along bays, such as the Qinzhou Bay, Dafeng River Estuary, and Fangcheng Bay, have severe environmental conditions (under level IV), and the most out-of-limit pollutants are dissolved inorganic nitrogen (DIN), active phosphate and oil, which are causing increasing detriment to the Beibu Gulf environment. The conditions of these items may affect the ecosystem in the gulf through transportation and biochemical processes. Studying the nutrient distributions, budget and flux is of great importance in providing a scientific perspective on the Beibu Gulf.

One way to study the subjects above is field investigations. Some field investigations concerning the water quality, biological processes, and distributions of ecological factors, such as nutrients, phytoplankton, zooplankton, benthic animals, and fish, have involved special periods and stations, showing that these factors have their own distribution characteristics and that the water mass exchange across the gulf and human activity along the estuaries may be critical (Cai et al., 2012; Chen et al., 2011; Fu et al., 2012; Liu et al., 1998; Tang et al., 2003; Wang et al., 2015; Zheng et al., 2014; Zhou et al., 2011). However, compared to those in the open SCS, field investigation data in the Beibu Gulf are relatively sparse (Bauer and Waniek, 2013). Moreover, outside the areas and periods of field investigations, many details have remained unknown, which makes some analyses difficult, especially quantitative analyses of the nutrient budget and flux.

Foundation item: The National Key Research and Development Program of China under contract No. 2017YFC1404801; the Program of Xiamen Southern Oceanographic Center under contract No. 15PZB009NF05.
*Corresponding author, E-mail: panwr@xmu.edu.cn

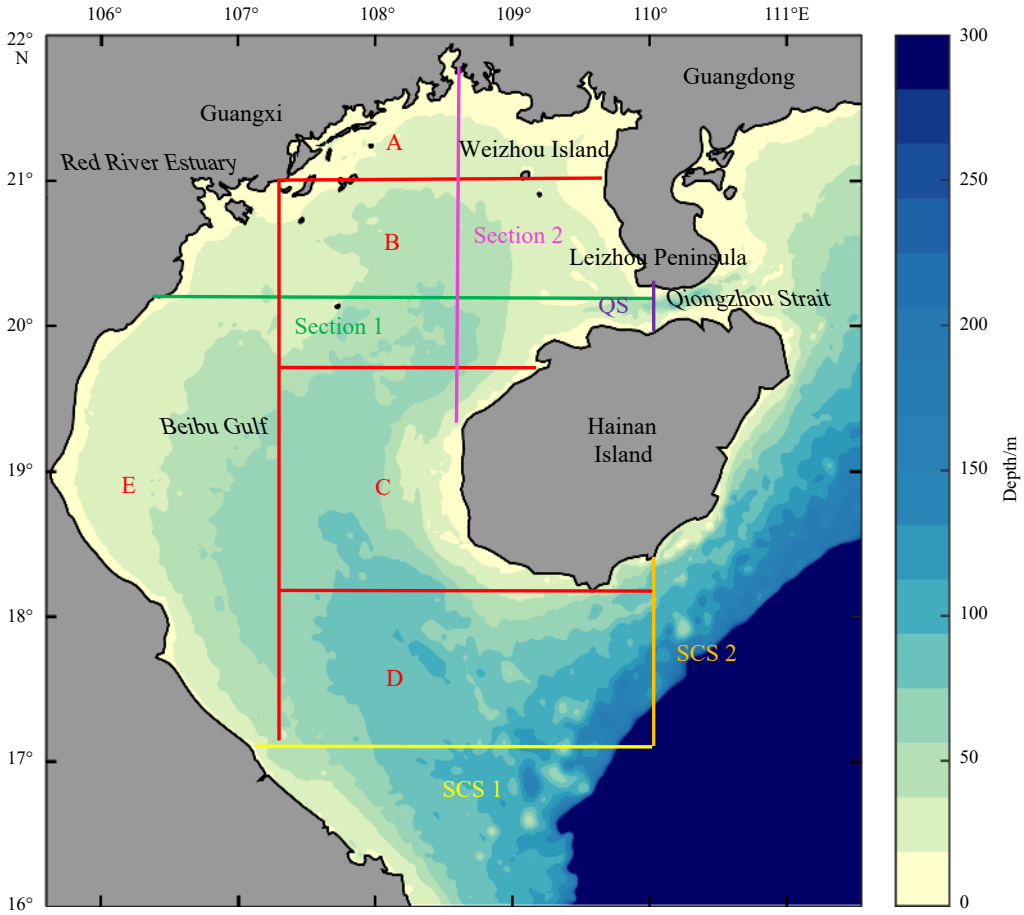

Fig. 1. The study domains of the model. The sections and boxes in the figure refer to the geographic locations of : the latitudinal section (Section 1) from the Red River Estuary to the Qiongzhou Strait and the longitudinal section (Section 2) from the Guangxi coast to the west of Hainan Island to show the vertical distribution patterns; boxes A, B, C, D and E to calculate the regional contributions of biochemical and physical processes to the nutrient budgets; the Qiongzhou Strait section (QS), the latitudinal section of South China Sea (SCS 1) and the longitudinal section of South China Sea (SCS 2) to calculate the nutrient flux across the gulf mouth.

A model is one of the effective ways to deepen analysis on the basis of field investigations. In addition, a coupled 3D hydrodynamic-ecological model is efficient for studying the hydrodynamic and ecological processes of an entire area throughout a time series (Fennel et al., 2006; Gan et al., 2010; Ianson and Allen, 2002; Wang et al., 2013a). Several ecological models have been applied in the SCS (Chai et al., 2009; Gan et al., 2010; Li et al., 2015; Liu and Chai, 2009; Liu et al., 2002). Bauer and Waniek (2013) used a 1-dimensional physical-ecological model to study the interactions between the associated physical water column structure, atmospheric forcing, and primary production within the entire seasonal cycle in the central part of the Beibu Gulf from 2000 to 2010. Additionally, the models applied in Beibu Gulf are mainly physical models used to study hydrodynamic circulation (Ding et al., 2013; Gao et al., 2014, 2013; Guo et al., 2015; Minh et al., 2014; Wang et al., 2018) and Ecosim models used to investigate ecological trophic structures (Chen et al., 2008, 2009b). It is essential to apply multidimensional biophysical models to more accurately study the spatial and temporal ecological distributions and channel effects in the Beibu Gulf.

The Marine Environment Commitee nutrient-phytoplankton-zooplankton-detritus (MEC-NPZD) hydrodynamic-ecological model can be a good choice. The 3D multilayer physical model of the MEC ocean model, which was developed by the Marine Environment Committee of Japan (2003), combines the global hydrostatic model with full-3D models for simulating currents on different spatial scales (Kano et al., 2010; Sato et al., 2006; Yu and Kyozuka, 2003). Its byproduct, the ecological nutrient-phytoplankton-zooplankton-detritus (NPZD) model, consists of eight major compartments: DIN, active phosphate (P-PO_4, which also refers to dissolved inorganic phosphorous, DIP, in this situation), phytoplankton, zooplankton and dissolved organic matter (DOM) and particulate organic matter (POM). This NPZD model uses the output of the current, temperature and salinity fields of the hydrodynamic model as input physical fields and can calculate key biological processes of a low-trophic level ecosystem, and it has solved some environmental and ecosystem problems in gulf or coastal areas (Nakata and Doi, 2006; Mizumukai et al., 2008; Hakuta and Tabeta, 2013; Wang et al., 2013b; Wang and Tabeta, 2017).

Therefore, to understand ecological characteristics such as the key regions, key periods and nutrient refreshment in the Beibu Gulf, the MEC-NPZD model was applied to simulate the spatial and temporal distributions of ecological variables throughout the entire gulf, quantitatively analyzed the contributions of individual processes to the nutrient budget in different regions, and calculated the nutrient flux between the Beibu Gulf and open SCS.

2 Method

2.1 *Hydrodynamic model*

The MEC model was applied to simulate the hydrodynamic conditions of the Beibu Gulf. In this model, the Mellor-Yamada 2.5 level turbulence closure model (Mellor and Yamada, 1982) was used to simulate the vertical eddy viscosity and diffusivity. The horizontal diffusion coefficients were calculated using the Smagorinsky turbulence closure model (Smagorinsky, 1963). The model can solve the hydrodynamic primitive equations using the hydrostatic assumption in the vertical direction with the Boussinesq simplification for convective flows.

The studied domain (Fig. 1) was divided into a 330 by 315 grid with a horizontal resolution of 2 km by 2 km and 10 levels (2.5 m, 7.5 m, 12.5 m, 17.5 m, 25.0 m, 35.0 m, 45.0 m, 55.0 m, 70.0 m, and 110.0 m depths) in the vertical direction according to Cartesian coordinates. The depth field in the domain was extracted from the ETOPO1 with a resolution of 1° by 1°. The detailed equations of the model have been described in Kano et al., 2010; Mizumukai et al., 2008; Sato et al., 2006, and the concrete model settings and validation have been described in Wang et al., 2018.

2.2 *Ecological model*

Based on the output physical fields of the hydrodynamic model, we used the NPZD model based on Nakata (1993) to simulate the distributions of the ecological variables (Fig. 2).

In the NPZD model, physical, biological, and chemical processes influence the ocean ecological distribution and processes, and the general equation is shown below:

$$\frac{\partial B}{\partial t} = -\left(u\frac{\partial B}{\partial x} + v\frac{\partial B}{\partial y} + w\frac{\partial B}{\partial z}\right) + A_c \cdot \left(\frac{\partial^2 B}{\partial x^2} + \frac{\partial^2 B}{\partial y^2}\right) + \frac{\partial}{\partial z}\left(K_c \cdot \frac{\partial B}{\partial z}\right) + \left(\frac{\partial B}{\partial t}\right)^*, \quad (1)$$

where B represents the ecological variables; thus, $\frac{\partial B}{\partial t}$ is the partial derivative of the ecological variables relative to time. u, v and w are the flow velocities in the x, y and z directions, A_c and K_c represent the diffusion coefficients in the horizontal and vertical directions, and $\left(\frac{\partial B}{\partial t}\right)^*$ is the biochemical source/sink term, representing the effect of the biochemical processes on the ecological variables relative to time, including the processes of phytoplankton (PHY), zooplankton (ZOO), DIN, DIP, cellular nitrogen (Q_N), cellular phosphorus (Q_P), POM, DOM and dissolved oxygen (DO).

The detailed functions of the NPZD model are described in the Supplemental Information. The parameters and their meanings as applied in the NPZD model are shown in Table S1.

In the model, biochemical processes include phytoplankton photosynthetic uptake, phytoplankton respiration, phytoplankton dead cellular release, zooplankton respiration, mineralization of organic matter and sediment dissolution, and the physical processes affecting the nutrient budget include the river input and the convective transport of the water. Performing integral operations on Eqs (3) and (4) in the Supplemental Information can yield the annual contributions of these processes to the DIN and DIP budgets and the annual flux of DIN and DIP in specified sections.

2.3 *Initial and boundary conditions*

The initial and boundary conditions included the tidal harmonics, daily averaged elevation, temperature, salinity, heat flux, wind data, sea surface temperature (SST), and monthly river discharge. The sources of these conditions are shown in Table 1.

The model was spun up with zero elevation and velocity, and the time step was set to 12 s for the hydrodynamic model and 60 s for the ecological model. The current, temperature and salinity fields of the ecological model were provided by the physical model. The model ran for 2 years, and the data from the latest year (2015) were exacted for analysis.

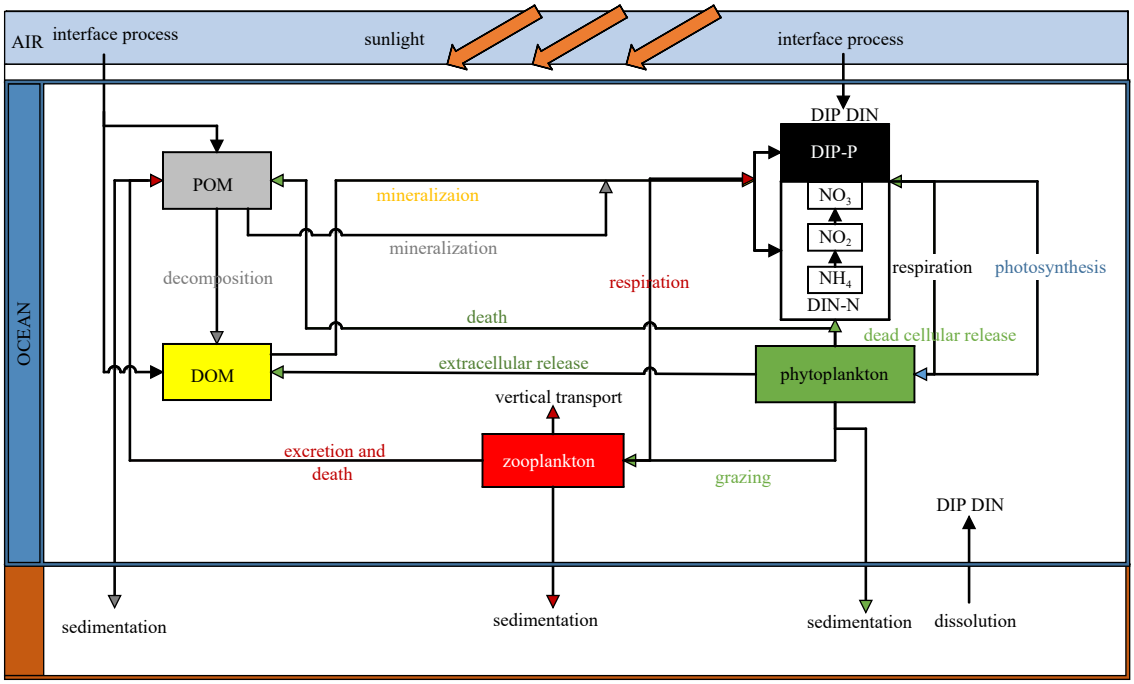

Fig. 2. NPZD model schematic.

Table 1. The sources of initial and boundary conditions

Data	Source	Resolution
Eight tidal (K_1, O_1, P_1, Q_1, M_2, S_2, N_2, K_2) Harmonics	Oregon State University tidal model	1 h
Daily average wind data	NOAA National Climatic Data Center (NCDC) Blended Sea Winds	0.25°×0.25°
Daily average heat flux	EU National Energy and Climate Plans (NECP)	1°×1°
Daily average SST	The Remote Sensing Systems (REMSS)	9 km/d
Elevation, temperature, salinity	Hybrid Coordinate Ocean Model (HYCOM)+Navy Coupled Ocean Data (NCODA)	(1/12)°×(1/12)°
Monthly river discharge	Gao et al., 2013; Han, 2013; Pruszak et al., 2005; van Maren and Hoekstra, 2004	–
Chl *a*	MODIS Aqua Monthly Average	4 km
NH_4, NO_2, NO_3, PO_4	World Ocean Atlas (WOA) 2014	1°×1°

The initial vertical distribution of Chl *a* in the water column was fitted by a Gaussian curve (Morel and Berthon, 1989). The initial phytoplankton biomass (mg/m^3, according to carbon) was set to 50 times the Chl *a* concentration (mg/m^3, according to carbon), and the initial zooplankton biomass was set to 5 times the Chl *a* concentration, respectively (Liu and Chai, 2009; Thomas and Dodson, 1972).

2.4 *Model validation*

The model with the field investigation and remote sensing data was validated. The field investigation data were from the Chinese Offshore Investigation and Assessment (COIA) hosted by the State Oceanic Administration of China in 2007, which was the largest field investigation of Chinese territorial waters in the Beibu Gulf in recent years. The sampling sites contained varying depths and seasons; thus, they are merged to the nearest model depths and representative months. The temperature, salinity, Chl *a*, DIN and DIP of the model result run for the year of 2007 were compared with the processed COIA data to validate the model system. The model simulated SST and phytoplankton (Chl *a*) distribution run for the year of 2015 were validated against remote sensing data (MODIS Aqua 4 km resolution) of the same year. The remote sensing data were transformed to 2 km resolution, which corresponds to the resolution of the model output.

3 Results

The physical and ecological variable distribution patterns in the Beibu Gulf were simulated and the nutrient budgets for different seasons and zones were analyzed. The data from January, April, July and October were used to represent winter, spring, summer and autumn in the studied region. As the average euphotic layer depth in the Beibu Gulf is nearly 12.5 m, the horizontal distribution data at 2.5 m and 12.5 m depth layers are shown to represent the sea surface and average euphotic layer of the gulf, respectively. Additionally, the vertical data from 10 layers across the latitudinal section (Section 1) from the Red River Estuary to the Qiongzhou Strait (20.2°N) and the longitudinal section (Section 2) from the Guangxi coast to the west of Hainan Island (108.6°E) (Fig. 1) and were interpolated for the study of the vertical distribution patterns.

3.1 *Model validation*

3.1.1 *Comparison with field investigation data*

Figure 3a is the map of the COIA stations in the Beibu Gulf.

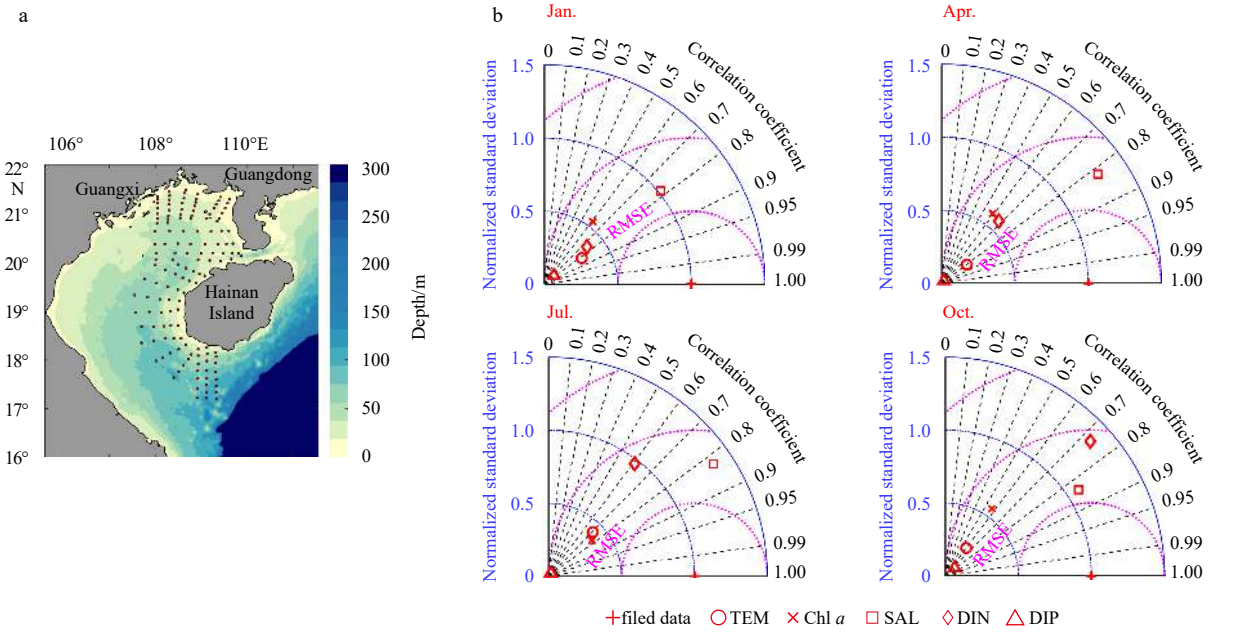

Fig. 3. The comparison with the field investigation data. a. Field investigation stations of the COIA in the Beibu Gulf in 2007; b. Taylor diagrams of the model simulated temperature (TEM), salinity (SAL), phytoplankton (Chl *a*), DIN and DIP and field data comparison in four seasons, with the STDs normalized to the observations (field data) and the RMSE between the simulated output and observation shown proportionally to their distance.

The sampling sites contained varying depths, and the sampling times were divided into four seasons. Figure 3b is the Taylor diagram (Taylor, 2001) for the comparison of the model results and observations (here, field investigation data), in which the correlation coefficients are above 0.6 for most model results, and the normalized standard deviations (STDs) are within 1.0 for all variables except the salinity (SAL) in all seasons, and DIN in autumn. However, the root mean square error (RMSE) shows that the model results for the four seasons are within a reasonable distance from the field investigation data (Peña et al., 2016; Jiang and Wang, 2018). The comparison validates the accuracy of the model system for various variables and depths.

3.1.2 *Comparison with remote sensing data*

Figure 4 is the Taylor diagram for the comparison of the data and observations (which here is the remote sensing data). The correlation coefficients of the SST and Chl *a* are above 0.8 in January, April and July and above 0.7 in October, meaning that the model results and remote sensing data have a high correlation. Considering the RMSE, the model results for January, April and July are closer to the remote sensing data compared to those for October. The normalized STDs of the model data are within 1.0, meaning that the model results had a smaller STD than that of the observations. However, the overall variation between the model results and remote sensing data for the SST and Chl *a* is within the acceptable error range (Tian et al., 2015). This comparison validates the accuracy of the model simulated results of 2015 at the sea surface of the studied domain.

Therefore, the model validation against both field investigation data and remote sensing data prove the accuracy of the model.

3.2 *Distributions of physical variables: temperature, current and salinity*

The horizontal distributions of the results of the physical variables are shown in Figs 5a, 5b, 6a and 6b.

In January, the current circulation at the 12.5 m layer is almost the same as that at the sea surface (2.5 m depth layer), except in the area of the southern gulf (17°–18°N, 108°E), in which the flow is westward on the surface and eastward at the 12.5 m depth layer. The temperature along the coast of the northern gulf is lower than that of the southern gulf. However, the temperature in the gulf is almost below 26°C. The temperatures and salinities of the two layers are almost identical.

In April, the southwest monsoon begins to take over the northeast monsoon, and the wind speed is slower than that in winter. However, the circulation is still cyclonic. The boundary flow of the open SCS intrudes into the gulf near 18.5°N and then

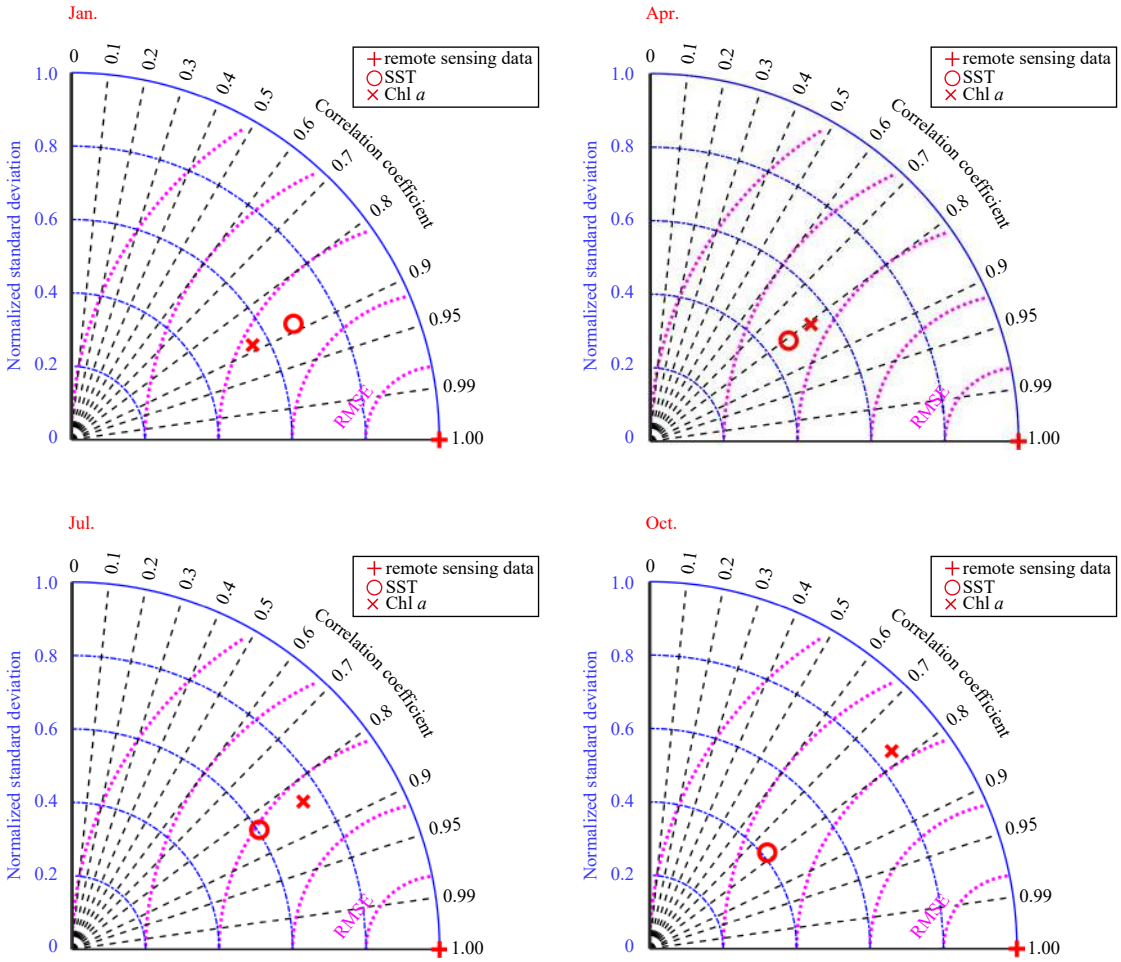

Fig. 4. Taylor diagrams of the model simulated and phytoplankton (Chl *a*) at 2.5 m depth and MODIS Aqua monthly average SST and Chl *a* data comparison, with the STDs normalized to the observations (MODIS Aqua data) and the RMSE between the model output and observations shown proportionally to their distance.

flows southward along the Vietnam coast, carrying the high-temperature open SCS water to the southern gulf. The temperature in the gulf increases significantly in spring, and the temperature difference in the gulf at this point is smaller than that in January. The average temperature at the 12.5 m depth layer is lower than that at the sea surface.

In July, the gulf is under the control of the southwest monsoon, and the current direction to the south of the gulf is northeastward or eastward. The current direction within the gulf is complex, with several gyres. There is a strong southward current along the Vietnam coast. The westward current in the Qiongzhou Strait becomes weaker in summer. The current speeds along the Qiongzhou Strait, the Vietnam coast and the southern gulf mouth are faster compared to those in the central gulf, and the current speed at the 12.5 m depth layer is slower than that on the sea surface. The temperature in the gulf is the highest in sum-

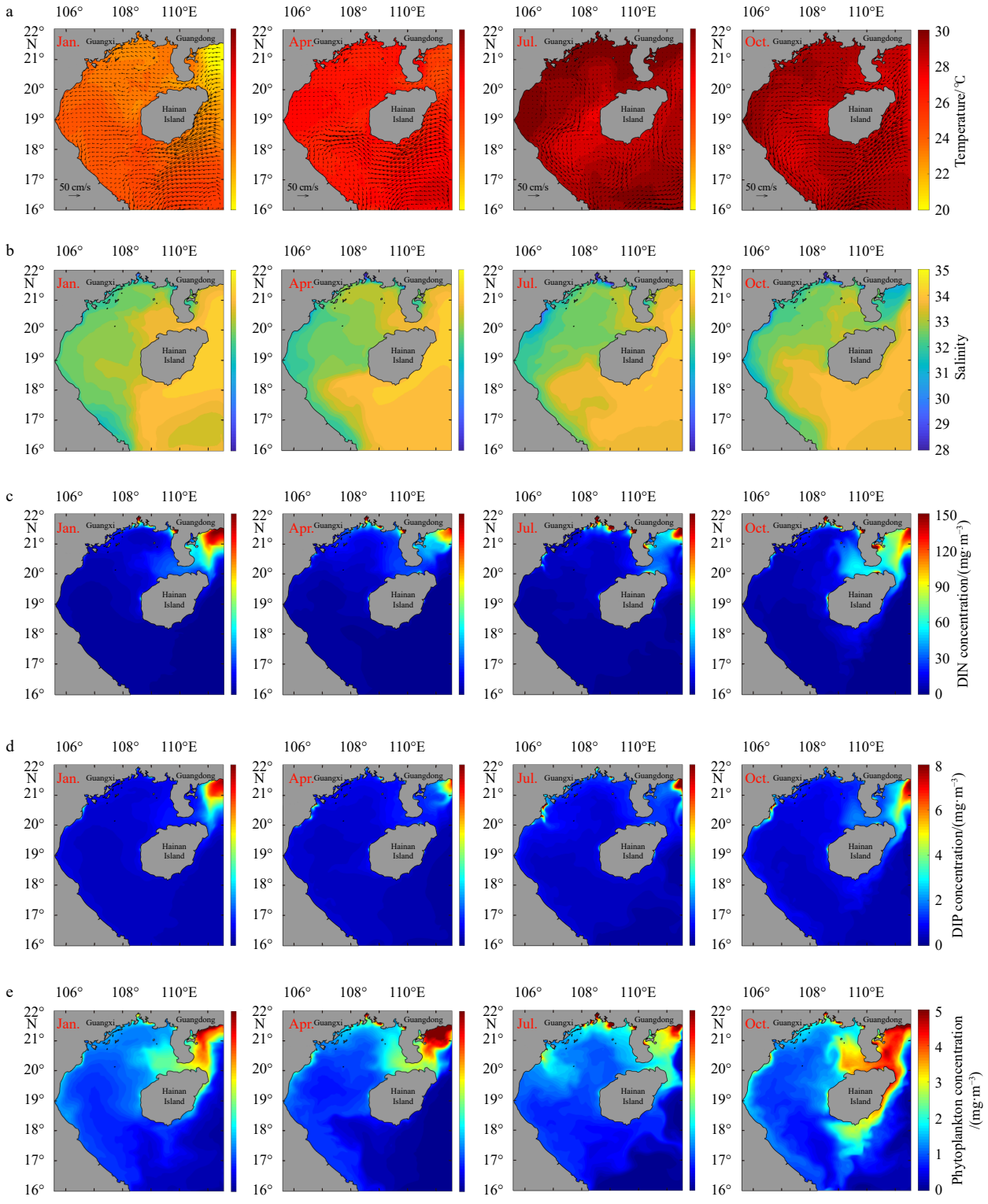

Fig. 5.

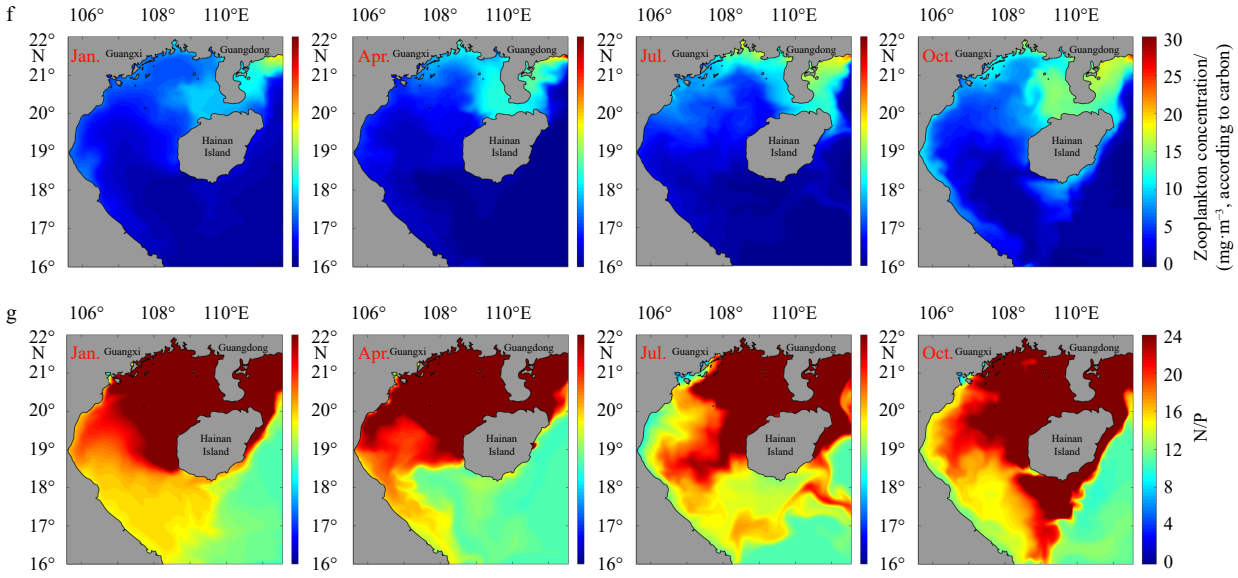

Fig. 5. Seasonal horizontal distribution of the variables at 2.5 m depth: temperature and currents (a); salinity (b); DIN (c); DIP (d); phytoplankton (e); zooplankton (f); N/P ratio (g).

mer, with some areas exceeding 30°C at the 2.5 m depth layer. The temperature at the 12.5 m depth layer is much lower than that on the surface. At the 12.5 m depth layer, the low-temperature areas are larger than those at the 2.5 m depth layer.

In October, the monsoon returns to the northeast monsoon, and thus, the current circulation becomes cyclonic again. The westward current in the Qiongzhou Strait is very strong at both the 2.5 m and 12.5 m depth layers. The temperature distribution difference throughout the entire gulf is less than 3°C. However, the temperature in autumn is higher than that in April in general, and the temperature and salinity differences between the two layers decrease than those in summer.

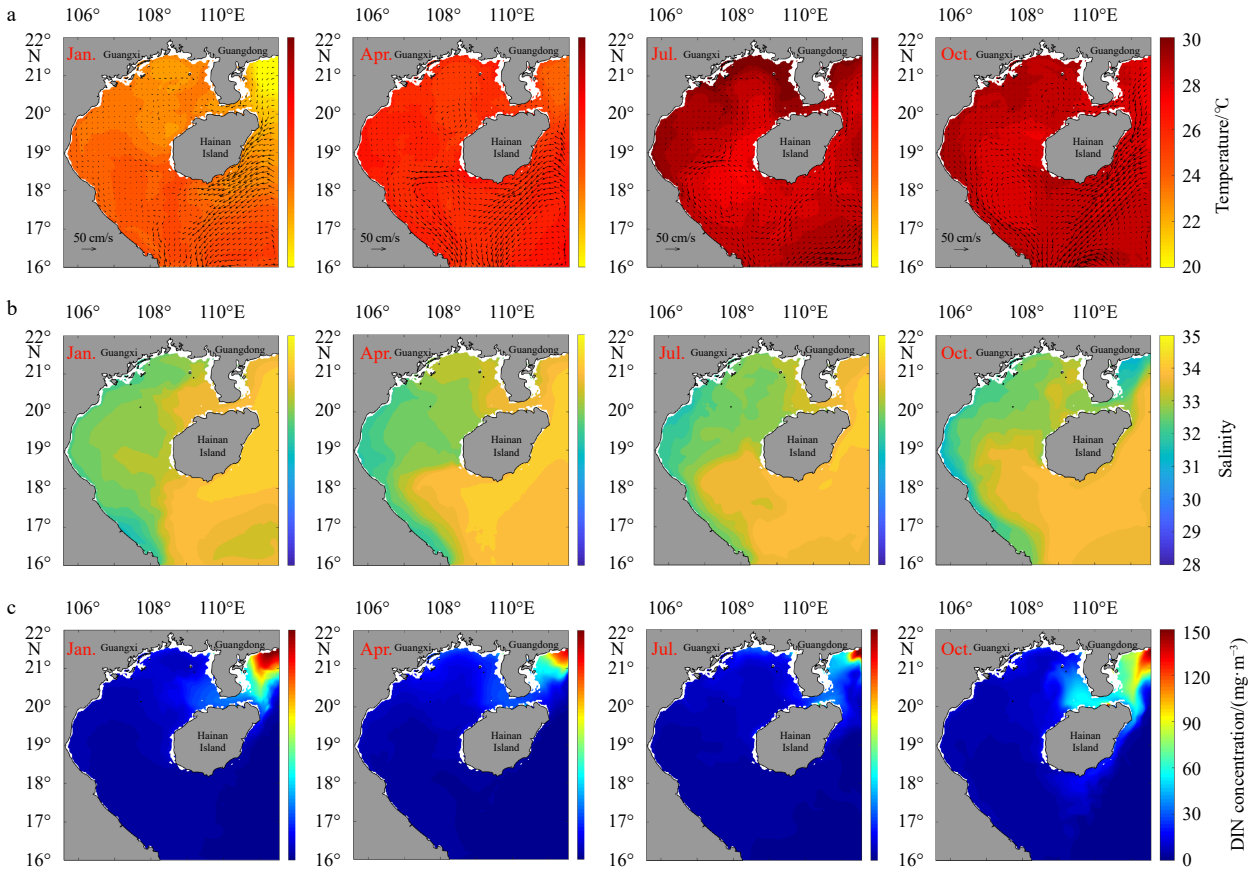

Fig. 6.

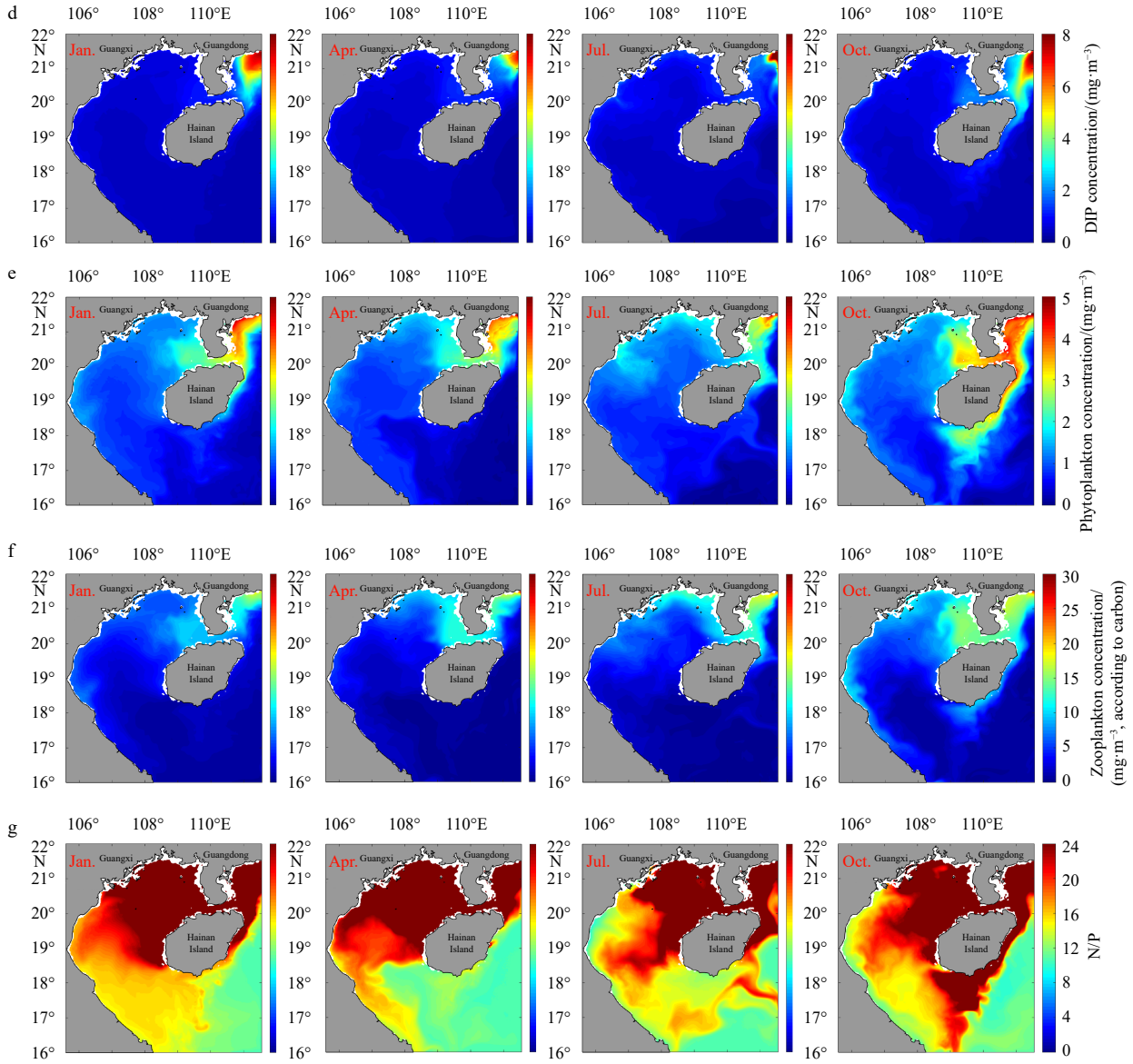

Fig. 6. Seasonal horizontal distribution of the variables at 12.5 m depth: temperature and currents (a); salinity (b); DIN (c); DIP (d); phytoplankton (e); zooplankton (f); N/P ratio (g).

In general, the salinity decreases from east to the west and from south to north, reflecting the current flow pattern in the gulf. The low salinity along the western and northern coasts of the gulf is due to the effect of river discharge, while the higher salinity near the southern gulf is the result of open SCS intrusion.

The vertical distribution results for the two sections are shown in Figs 7a, 7b, 8a and 8b. In these two sections, the temperature is lower at the bottom of the central gulf. The temperature and salinity stratifications are more obvious in spring and summer. At the bottom of the central gulf, there are obvious low-temperature water areas in April and July.

The high-salinity areas of Section 1 in winter are in the west of the Qiongzhou Strait to the central gulf, and the stratification effect is small. The high-salinity areas of Section 2 exist in the central gulf, north of Hainan Island.

The average vertical distributions of the temperature differences in the four representative months are similar to the horizontal distribution. The temperature is lower at the sea bottom of the central gulf due to bathymetric conditions. However, the temperature stratification is more obvious in summer when the temperature is higher than in other seasons.

3.3 *Distribution of nutrients: DIN and DIP*

The horizontal distributions of the DIN and DIP are also shown in Figs 5c, 5d, 6c and 6d. The distribution characteristics of the DIN and DIP decrease from the east to west, onshore to offshore, and north to south in general. The distributions of the DIN and DIP are strongly influenced by interface processes.

In January, when the prevailing northeast monsoon makes the westward transport of water in the Qiongzhou Strait strong, the DIN concentration to the west of the Qiongzhou Strait can reach as high as 50 mg/m^3, and the DIP concentration is higher than 2 mg/m^3. In April and July, areas with high DIN and DIP concentrations appear in estuaries. In October, the northeast monsoon returns, the nutrient supplementation from the Qiongzhou Strait reaches the northern gulf, and the nutrient concentration to the west of the Leizhou Peninsula can reach as high as

50 mg/m^3 for the DIN and 3 mg/m^3 for the DIP.

The distribution characteristics of the DIN and DIP at the 12.5 m depth layer are similar to those at the 2.5 m depth layer.

In the vertical distribution view (Figs 7c, 7d, 8c and 8d), the DIN and DIP concentrations at the bottom of the central gulf are higher than those in spring and summer.

3.4 *Distribution of biological variables: phytoplankton and zooplankton*

The horizontal distribution results indicate that the general concentrations of phytoplankton (Figs 5e and 6e) and zooplankton (Figs 5f and 6f) decrease from east to west, onshore to offshore, and north to south, following the distribution of inorganic nutrients. This is the same trend shown in field studies (Van Thuoc et al., 2012; Liu et al., 1998; Wang et al., 2015) and remote sensing data (Tang et al., 2003).

In January and October, areas with high phytoplankton (>2 mg/m^3) and zooplankton (>10 mg/m^3, according to carbon) concentrations exist near the western coast of the Leizhou Peninsula. In April and July, the areas with high phytoplankton and zo-

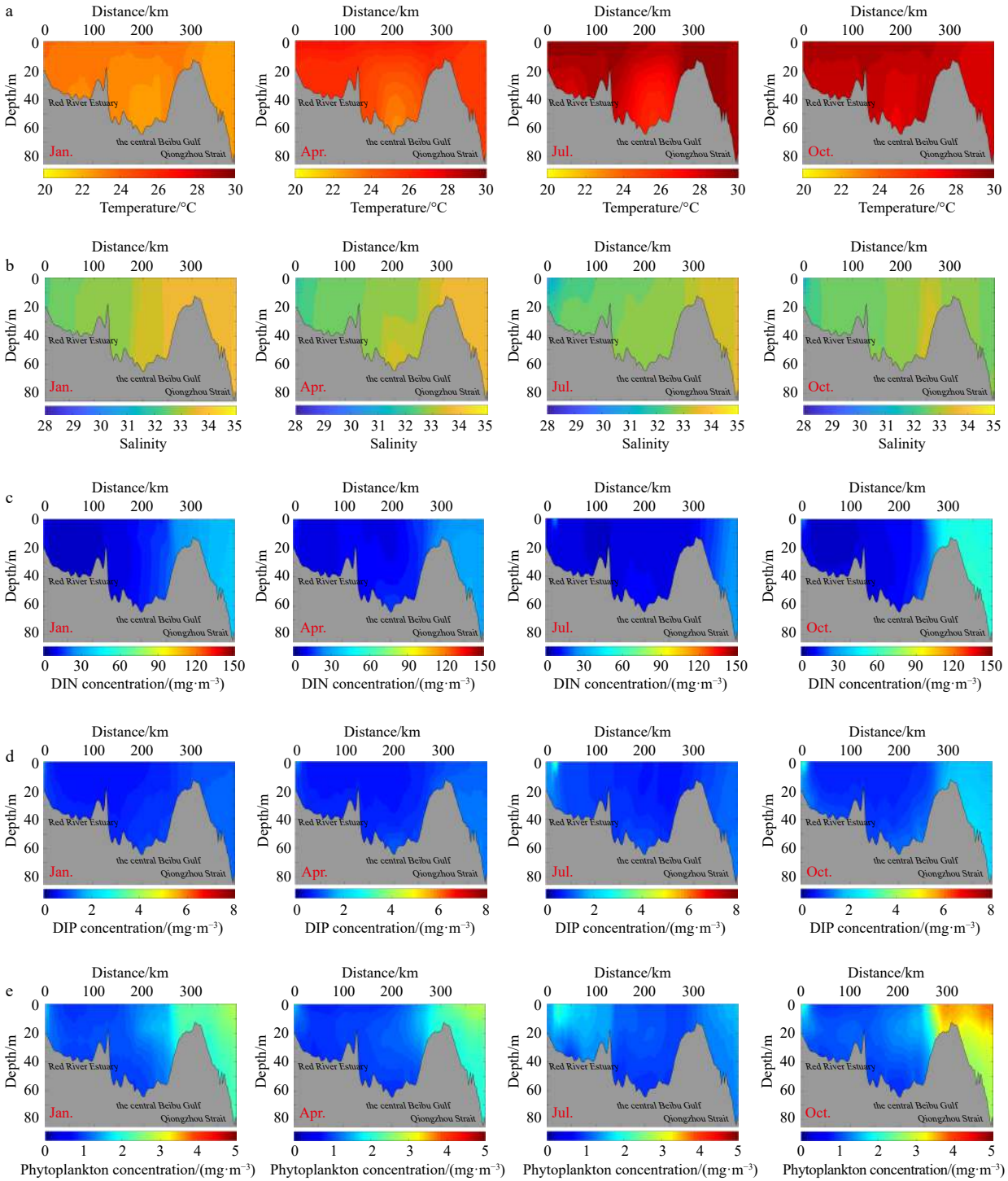

Fig. 7.

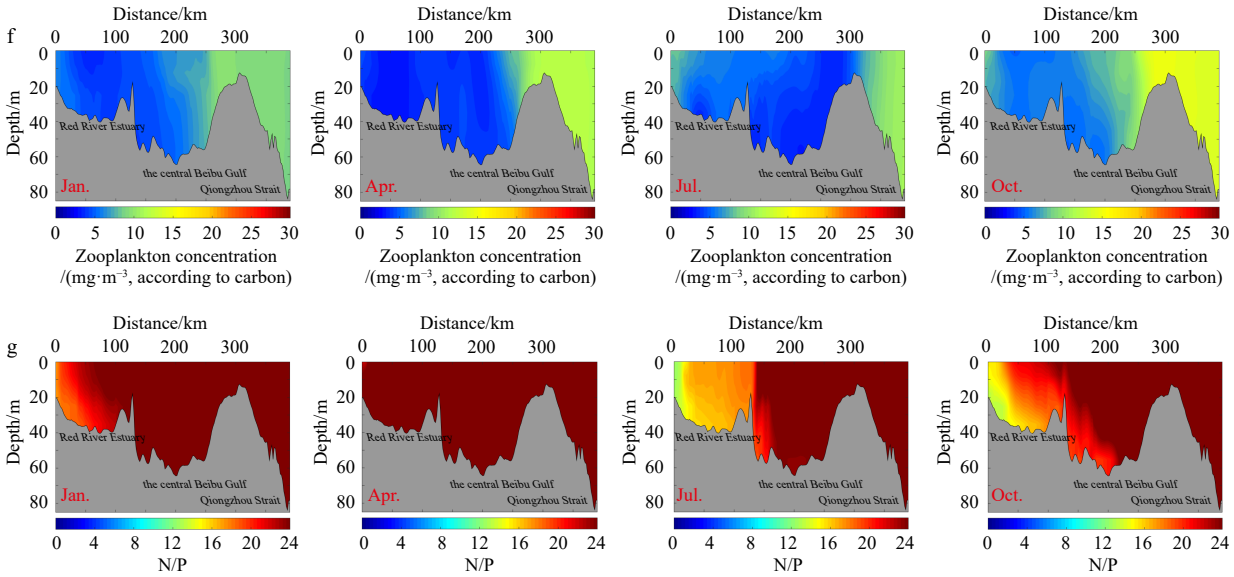

Fig. 7. Seasonal vertical distributions of the variables in Section 1: temperature (a); salinity (b); DIN (c); DIP (d); phytoplankton (e); zooplankton (f); N/P (g).

oplankton concentrations shrink towards the shore of the Leizhou Peninsula. At the same time, the concentrations of phytoplankton and zooplankton increase in the estuaries.

The phytoplankton and zooplankton distribution characteristics at the 12.5 m depth layer are similar to those at the 2.5 m depth layer but with somewhat lower values.

The vertical distribution of phytoplankton is shown in Figs 7e and 8e. Similar to the surface distribution, the areas with high concentrations of phytoplankton in January and October are located in the Qiongzhou Strait and to the west of the Leizhou Peninsula. In addition, a higher phytoplankton concentration area exists 10–20 m below the sea surface. The vertical zooplankton

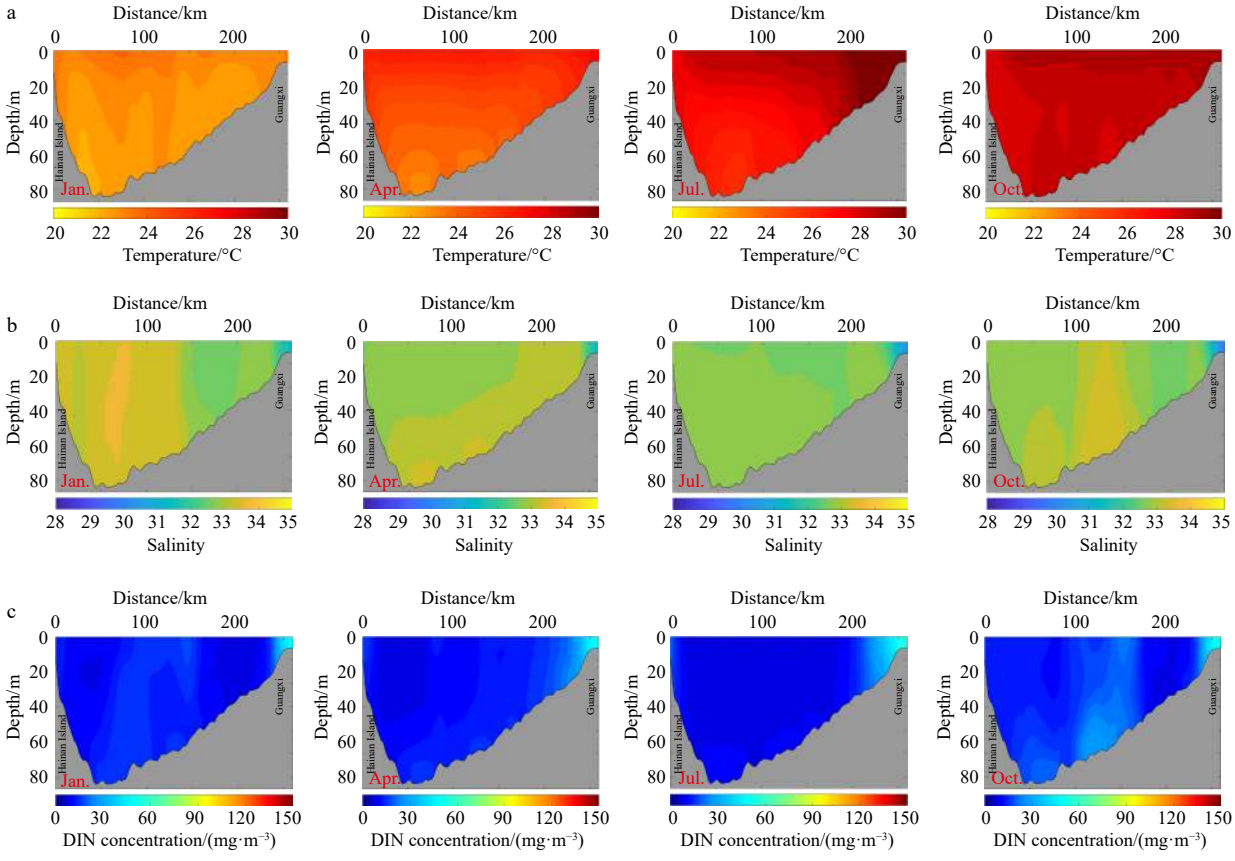

Fig. 8.

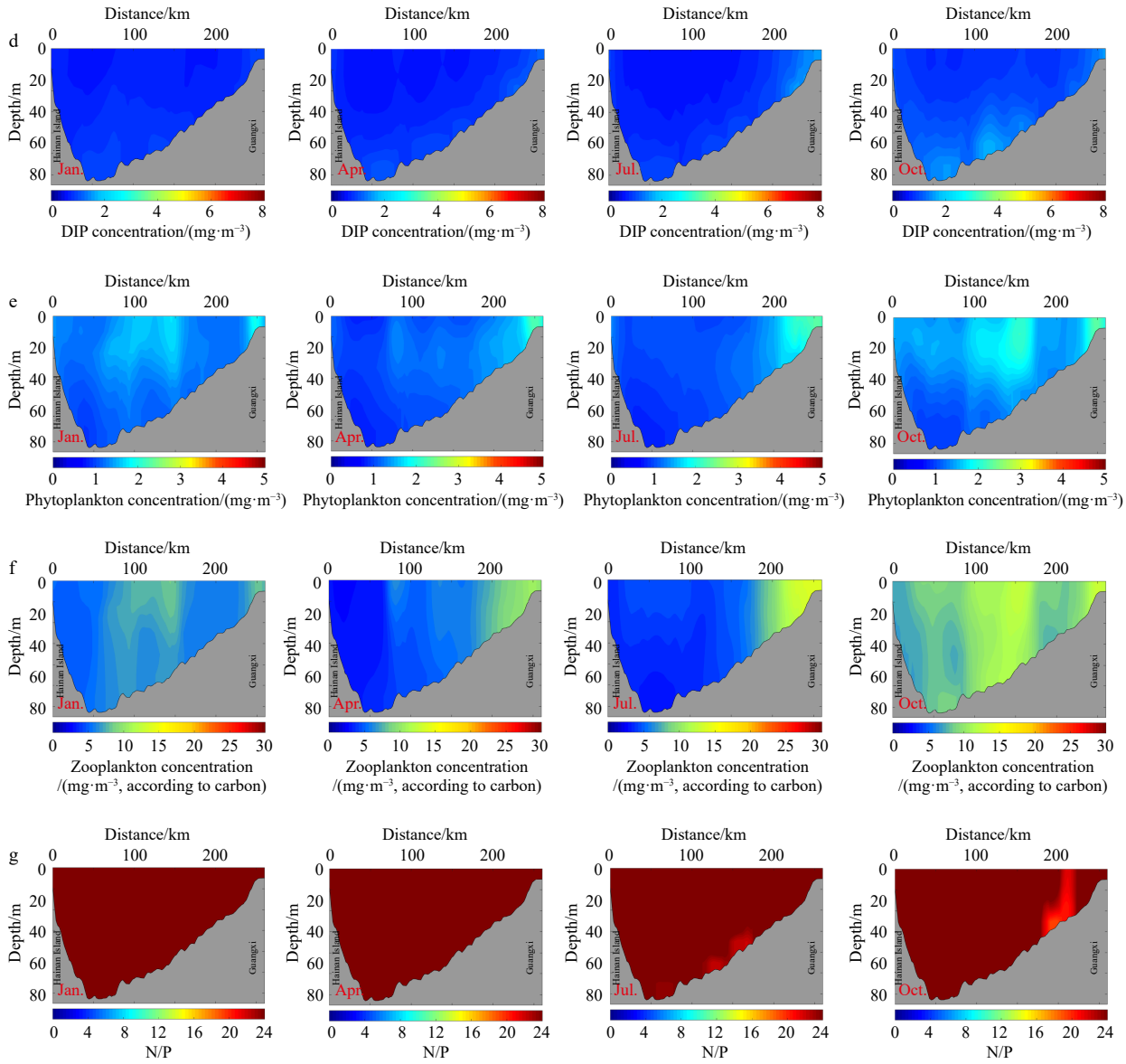

Fig. 8. Seasonal vertical distributions of the variables in Section 2: temperature (a); salinity (b); DIN (c); DIP (d); phytoplankton (e); zooplankton (f); N/P (g).

distribution (Figs 7f and 8f) is similar to that of phytoplankton, but the areas with high concentrations of zooplankton can be deeper than those of phytoplankton.

3.5 *Contributions of processes to the DIN and DIP*

The annual budgets of processes for the DIN and DIP are shown in Fig. 9, and the annual budget changes of biochemical and physical processes for the DIN and DIP are shown in Fig. 10.

Phytoplankton uptakes 1 761 700 t of DIN and 221 730 t of DIP annually. Phytoplankton respiration and phytoplankton dead cellular release supply 400 068 t of DIN and 66 679 t of DIP, making them the largest nutrient sources. Mineralization is also an important source of nutrients, which contributes 33 745 t of DIN and 56 291 t of DIP.

In the DIN budget, the contributions of most processes except river input and convective transport decrease from February to June and increase from July to December. However, sediment dissolution is more significant in summer and autumn, exceeding the process of zooplankton respiration. Phytoplankton photosynthetic uptake is a sink of DIN for the water, and phytoplankton dead cellular release, phytoplankton respiration and mineralization are three main contributors to the DIN source, contributing 31.10%, 22.34% and 18.90% of the DIN source, respectively.

Similar to the DIN budget, most processes contributing to DIP decrease from February to June and increase from July to December, but the rates of decrease exceed the rates of increase. Sediment dissolution is more active in summer and autumn compared to zooplankton respiration and phytoplankton dead cellular release. Phytoplankton photosynthetic uptake is also a sink of DIP. The main contributors to the DIP source are phytoplankton respiration (29.92%) and mineralization (25.25%).

3.6 *Nutrient budget in different zones*

Figure 11 shows the biochemical and physical contributions to the budgets of the DIN and DIP in different zones, in which the

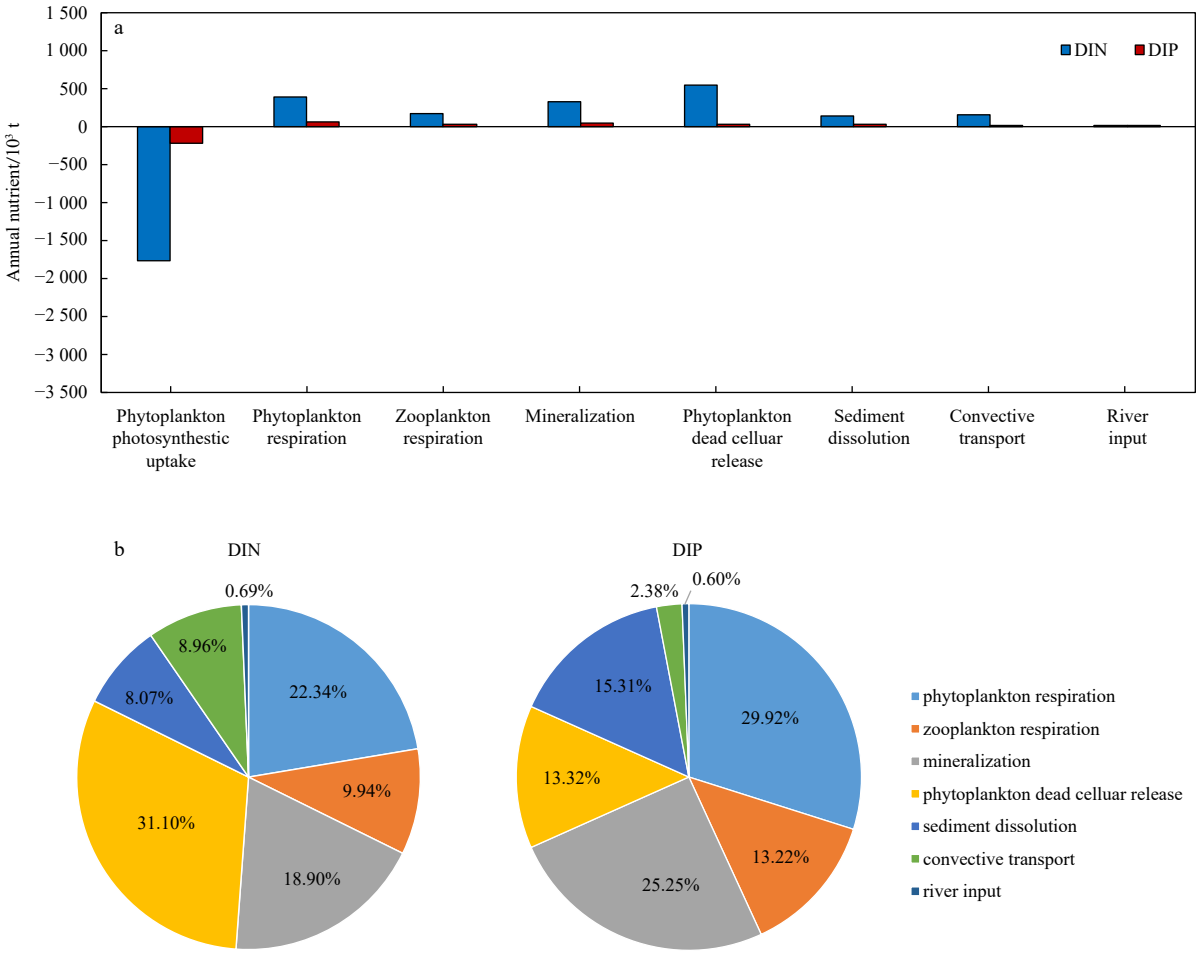

Fig. 9. The annual nutrient budgets of different processes: total budgets of the DIN and DIP (a); the contribution portion of each process to the DIN and DIP source (b).

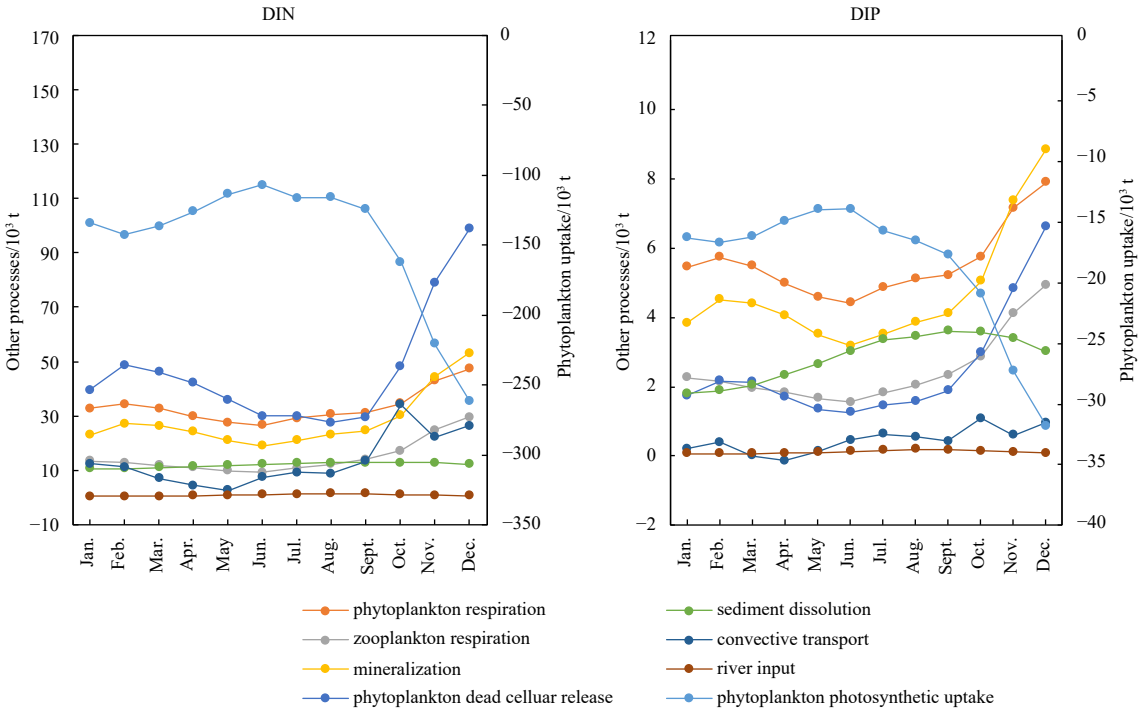

Fig. 10. The annual budget changes of different processes relative to the DIN and DIP.

data have been normalized to the zone areas. The results indicate that only phytoplankton photosynthetic uptake is a nutrient sink for the water in all zones, and the other processes are nutrient sources. Box B has the highest nutrient refreshment efficiency in general.

In Box A, the phytoplankton dead cellular release can contribute 41.89% of the DIN source, while mineralization provides the biggest supplement of DIP, which can contribute 23.22% of the DIP source. Box B has the largest photosynthetic uptake of both DIN and DIP. Phytoplankton dead cellular release is also the main source of DIN in Box B, which contributes 44.43% of the DIN source. For the DIP, the allocation proportion is similar to that in Box A, with mineralization taking first place. In Box C, the main source of DIN is phytoplankton respiration, followed by phytoplankton dead cellular release, which contribute 28.18% and 24.61% of the total DIN source in this zone, respectively. The main source of DIP in Box C is phytoplankton respiration, followed by mineralization. The allocation proportions of Box D are similar to those in Box C. In Box E, the largest DIN source is phytoplankton respiration, which contributes 28.30% of the DIN source, followed by mineralization (21.31%). Phytoplankton respiration also contributes the highest portion (30.54%) to the DIP source.

Compared to biochemical processes, physical processes contribute less to the nutrient budget. River input only contributes 2.19%, 0.38% and 1.68% of the DIN source and 2.20%, 0.19%, and 1.71% of the DIP source in Boxes A, C and E. Convective transport only contributes significantly in Box A and Box B. In other boxes, the contributions to nutrient sources by convective transport are negligible.

3.7 *Nutrient flux*

The nutrient flux in the water-exchange sections was calculated. The three sections in 110°E of the Qiongzhou Strait, in 17°N and 110°E of the southern gulf mouth (Fig. 1) were set. The annual transports of these sections are shown in Fig. 12.

The nutrient flux in the Qiongzhou Strait is westward into the gulf year-round. The amount is higher in winter and autumn and lower in spring and summer. The maximum DIN and DIP fluxes happen in December, with values of 24 606 t for DIN and 1 010 t for DIP. Moreover, the DIP consumed by phytoplankton is a larger portion than that of the DIN in autumn, so DIP transport cannot reach as sharp of a peak compared to that of DIN.

The DIN and DIP fluxes in the latitudinal section of the southern gulf mouth (17°N, SCS1) are southward into the open SCS year-round, and in winter and autumn, the southward nutrient fluxes increase. In spring, the southward nutrient fluxes decrease under the influence of the southwest monsoon. The maximum transports of both the DIN and DIP occur in December.

The fluxes of the DIN and DIN in the longitudinal section (110°E, SCS2) year-round are westward into the gulf.

4 Discussion

4.1 *Variable distribution*

Controlled by the northeast monsoon in winter and autumn, the current circulations during October and April are cyclonic in general, which corresponds to the results of another study (Wu et al., 2008). Although there are controversies concerning the current circulation in summer, recent studies revealed that the circulation structures remain cyclonic in most areas (Chen et al.,

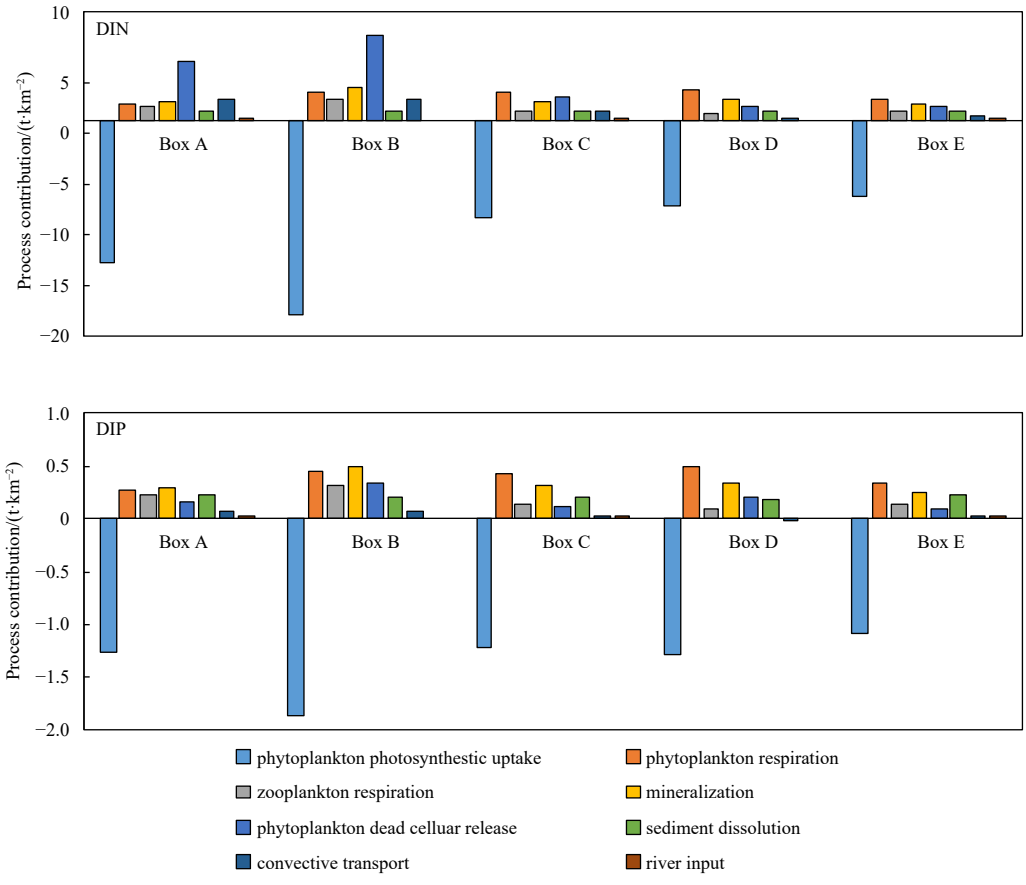

Fig. 11. Contributions of different processes to the DIN and DIP in different boxes.

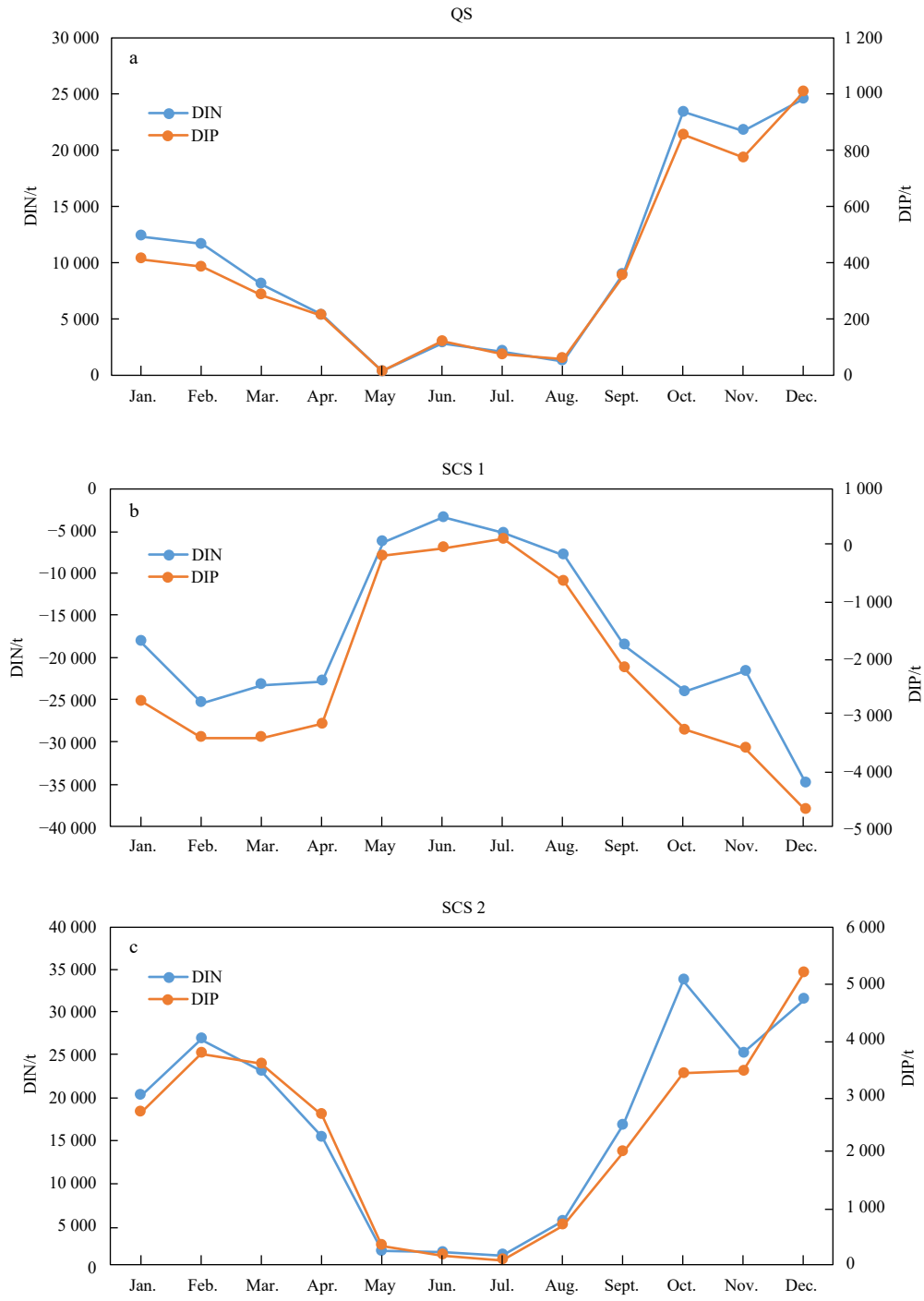

Fig. 12. Nutrient fluxes across the three sections: the Qiongzhou Strait section (QS), the latitudinal section of South China Sea (SCS 1) and the longitudinal section of South China Sea (SCS 2).

2015; Gao et al., 2013; Wang et al., 2018; Wu et al., 2008), which is also consistent with the model results. The results of the model and other studies show that the current direction in the Qiongzhou Strait is westward throughout the year; however, influenced by the direction of the monsoon, the westward velocity is greater in winter and smaller in summer (Chen et al., 2009a; Wang et al., 2018), so the westward water transport in the Qiongzhou Strait plays a critical role in the circulation of the Beibu Gulf (Wu et al., 2008). There is an upwelling current along western Hainan Island, coinciding with the occurrence of the strong current intrusion by the open SCS and the along-coast current from the north. Additionally, there are strong tide-mixing effects, and the mixing effects give this area the shortest retention time of modeled water particles (Hu et al., 2003; Kuo et al., 2000; Wang et al., 2018). Due to the intensity of the vertical water mixing, the temperature and salinity stratifications of the sea water in spring and summer are more apparent than that in winter and autumn, especially at the bottom of the central gulf, similar to the descriptions in other literatures (Chen et al., 2015; Ding et al., 2013; Gao et al., 2013). The hydrodynamic conditions form the background

for ecological modeling.

The ecological model simulated the distribution characteristics of nutrients, followed by Chl *a* and zooplankton, which decrease from east to west, onshore to offshore, and north to south in general, reflecting the seasonal patterns of the monsoon, river inputs and water exchanges in the gulf.

Cheng et al. (2017) found that the sediment concentration is higher in the Qiongzhou Strait, west of Hainan Island and along the coast of Vietnam and the Leizhou Peninsula using the ROMS model , and this characteristic may also contribute to the distribution of nutrients. In winter and autumn, nutrients from western Guangdong (Zhujiang River Estuary) are carried by the northeast monsoon through the Qiongzhou Strait into the Beibu Gulf (Bao et al., 2005), leading to a phytoplankton bloom near the west of the Leizhou Peninsula. The sediment-dissolving activities are strong in winter and autumn, so the DIN and DIP concentrations at the bottom of the central gulf are higher than those in spring and summer. Summer is the wet season in the studied region, in which the river inputs reach their maximum, carrying large amounts of nutrients into the gulf (Deetae and Wisespongpand, 2001; Lai et al., 2014; Zheng et al., 2012). In addition, due to the changes in the monsoon, the water with high-nutrient concentrations in the northern gulf cannot be diffused toward the south, making the high-nutrient areas limited among nearshore areas in the summer. During this period, high-concentration phytoplankton areas also exist in estuaries. Additionally, the growth rate of phytoplankton is higher than the grazing rate of micro zooplankton along the Guangxi coast in summer; therefore, phytoplankton can accumulate in this area. In contrast, to the south of Weizhou Island, the primary production is low, and the grazing effect becomes the key factor controlling the growth of phytoplankton (Ma et al., 2014). To the northwest of Hainan Island, there is a high-concentration phytoplankton area but no obvious high-concentration zooplankton area, which is not parallel to the high concentration of nutrients or phytoplankton here. This area is an upwelling region, so the nutrient concentration is high there. However, it is also a tidal mixing region, and the tabulated water mixing region might not be a favorable zone for zooplankton assembly.

The vertical distribution also indicates that the phytoplankton has strong correlations with the temperature, illumination intensity and nutrients beneath the sea surface. From summer to autumn, in addition to the stratification effect, the SST may exceed the optimum growth temperature for most phytoplankton; therefore, the higher phytoplankton concentration areas in the central gulf exist 10–30 m below the sea surface. The nutrient effect also plays an important role in the vertical distribution of phytoplankton, but it has less influence than do the temperature and illumination, especially beneath the sea surface. In autumn, the water flux in the Qiongzhou Strait is at its maximum throughout the year due to the substitution of the northeast monsoon. Additionally, the temperature near the west of the Leizhou Peninsula is fit for phytoplankton growth (<28°C), and the high-concentration phytoplankton area appears again to the west of the Leizhou Peninsula. Moreover, as the northeast monsoon becomes stronger, the high-concentration phytoplankton area in the Red River Estuary moves southward. The vertical distribution pattern of zooplankton follows the distribution pattern of phytoplankton, which is higher along coast and in the northwestern gulf and lower in the central and southern gulf. However, zones with high concentrations of zooplankton can be deeper than those of phytoplankton due to the sinking activities of zooplankton.

When the N/P ratio is calculated, most areas of the gulf are P-limited (Figs 5g and 6g); however, in the southern gulf, where water from the open SCS intrudes, the N/P ratio is under 16 or near 16, and this phenomenon is even more evident in summer because the current from the open SCS becomes stronger at this time. Field investigations have also revealed that the Beibu Gulf is a high-N/P region, and most areas of the gulf are P-limited (Wang et al., 2015; Yang et al., 2015). According to the study of Wang et al. (2015), the high-N/P area in the northern gulf can be attributed to the growth of diatoms because diatoms are the dominant phytoplankton in this region. The other reasons may be the large amount of nitrogen discharge from rivers in Guangxi (Lai et al., 2014). However, the N/P ratio along the Vietnam coast is under 16 in summer, especially in the Red River Estuary, indicating that the nutrient discharges from the Red River may include an increased amount of phosphate (Le et al., 2010), and then the southward alongshore current carries the nutrients down to the Vietnam coast. Additionally, the high-N/P area in the northern gulf retrenches from spring to summer, and this may be due to the effect of the water mass transport from the central gulf driven by the monsoon.

4.2 *Nutrient budget*

The biochemical processes of each box are stronger in autumn and winter; thus, autumn and winter are key seasons for phytoplankton growth, as well as mineralization. Concerning the biological activities of phytoplankton, Box B has the strongest activity, and its photosynthetic uptake of nutrients overwhelms the other four regions. Box A, which is located along the estuary of the Guangxi coast, has a significant increase of phytoplankton activity in summer, reflecting the distribution characteristics of phytoplankton, zooplankton and nutrients. In addition, the proportions of nutrient uptake and release vary in different boxes. For the DIN, except for the process of phytoplankton dead cellular release, the uptake and release of each box is more similar, and for the DIP, the process of sediment dissolution is more obvious in Box A.

Among the contributions of biochemical and physical processes to the nutrient budget, phytoplankton plays an important role in nutrient refreshment, as photosynthetic uptake is the biggest nutrient sink, while phytoplankton dead cellular release is the biggest nutrient source.

Compared with biochemical processes, physical processes contribute less to the nutrient budgets, but they play nonnegligible roles. For convective transport, the Qiongzhou Strait is an important channel for water exchange between the Beibu Gulf and open sea, and it contributes more to Box A and Box B. Box D is also connected to the open SCS, so it has a significant convective diffusion effect. In addition, for the river input process, Box A containing the estuary along the Guangxi coast and Box E containing the estuary along the Vietnam coast have significant river inputs. Box C, which includes the Changhua River input from the west of Hainan Island, exports fewer nutrients. This may be due to the lower water volume of runoff from the Changhua River.

When the annual nutrient budgets were calculated, the DIN and DIP of the four boxes in the eastern gulf increased, while the DIN increased and the DIP decreased in Box E (Fig. 13).

According to the results of the model, the nutrient flux direction of the Qiongzhou Strait is from east to west, and the channel between the Beibu Gulf and the open SCS is from east to west and north to south (Fig. 12). The higher nutrient flux in winter and autumn and lower nutrient flux in spring and summer in the Qiongzhou Strait are consistent with the water flux in this area

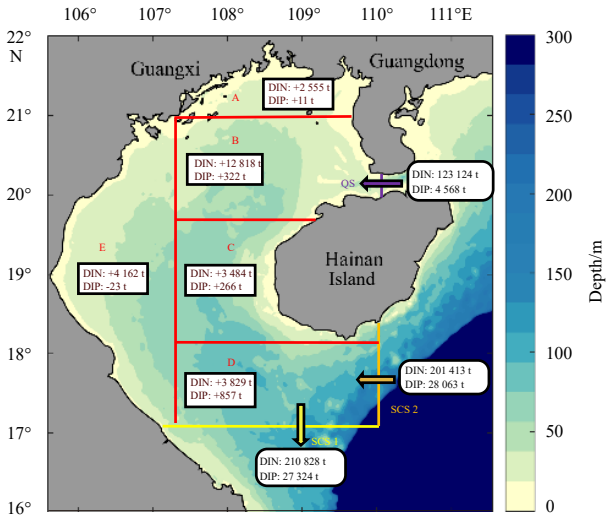

Fig. 13. Annual total nutrient budgets of the boxes and sections.

(Gao et al., 2013; Shi et al., 2002; Wang et al., 2018). This could also explain the area of high phytoplankton concentrations to the west of the Leizhou Peninsula in autumn and winter. In summer, as the southwest monsoon prevails, the westward water flux in the Qiongzhou Strait becomes weaker, as does the nutrient flux. Additionally, the nutrient flux in the model also reveals that the Qiongzhou Strait is a P-limited area, rather than a N-limited area, which is consistent with the N/P results here (Figs 5g, 6g and 7g).

The net nutrient input from the Qiongzhou Strait to the Beibu Gulf is 124 123 t for DIN and 4 568 t for DIP; the net nutrient output from the southern gulf to the open SCS in the latitudinal section (SCS1) is 210 828 t for DIN and 27 324 t for DIP; and the net nutrient input from the southern gulf to the open SCS in the longitudinal section (SCS2) is 201 413 t for DIN and 28 063 t for DIP (Fig. 13). Therefore, 9 415 t of DIN was exported to the open SCS from the southern gulf and 739 t of DIP was imported from the open SCS to the southern gulf in 2015. In summary, 113 709 t of DIN and 5 277 t of DIP are imported from the open SCS to the Beibu Gulf.

5 Conclusion

The distributions of ecological variables in the Beibu Gulf were simulated using the MEC-NPZD model, and the comparison of the results with field investigation and remote sensing data indicates that the model is able to simulate the ecological characteristics and analyze the nutrient budget in the Beibu Gulf for the year 2015.

Interface processes (monsoon, water flux, and river input) significantly influence the ecosystem in the Beibu Gulf. The concentrations of nutrients, phytoplankton and zooplankton are generally higher in the eastern and northern gulf and nearshore areas than in the western and southern gulf and offshore areas, and the difference between the sea surface layer (2.5 m depth) and the average eutrophic depth layer of the gulf (12.5 m depth) is slight.

In autumn and winter, a great amount of nutrient-rich water from the western Guangdong coastal area passes through the Qiongzhou Strait and flows into the Beibu Gulf, leading to intensified phytoplankton and zooplankton activities to the west of the Leizhou Peninsula. In summer, more nutrients come from rivers, and thus, high nutrient and Chl *a* concentrations appear in estuaries.

For the same reason, the nutrient flux between the Beibu Gulf and the open SCS is highly correlated with the monsoon and water flux. For the Qiongzhou Strait, the nutrient flux is from east to the west year-round but decreases from late spring to summer due to the changing direction of the monsoon, and the annual nutrient flux from the Qionzhou Strait to the Beibu Gulf is 123 124 t for DIN and 4 568 t for DIP. For the latitudinal section of the southern gulf mouth, the annual nutrient flux is from the gulf to the open SCS, while for the longitudinal section, the nutrients flow from the open SCS to the Beibu Gulf. Due to the varied flux of the DIN and DIP, the annual flux of DIN is 9 415 t from the southern gulf to the open SCS, while that of DIP is 739 t from the open SCS to the southern gulf. In general, the nutrient flux from the open SCS to the Beibu Gulf is larger in autumn and winter and smaller in spring and summer.

The nutrient budget and flux reveals that phytoplankton plays an important role, as follows: (1) photosynthetic uptake is the largest nutrient sink; (2) dead phytoplankton cellular release is the largest DIN source, contributing 31.10% of the DIN source, while phytoplankton respiration is the largest DIP source, contributing 29.92% of the DIP source; and (3) mineralization also provides a considerable supplement of inorganic nutrients, and it contributes 18.90% of the DIN source and 25.25% of the DIP source. Overall, biochemical processes have a greater influence on the nutrient budget in the Beibu Gulf compared to physical processes. When considering the nutrient budget in different boxes, the DIN and DIP in the four boxes of the eastern gulf show an annual increase.

According to themodel results, for the central and northern gulf, the key region is the Qiongzhou Strait, and the key periods are autumn and winter. For nearshore areas, the key regions are estuaries along the Guangxi coast in China and the Red River in Vietnam, and the key period is summer. The results may provide insight for use in environmental and regionalization management in the gulf.

Acknowledgement

We thank Longzhan Huang, Yifei Zheng, Lina Wang and Longlong Zeng for providing suggestions to build the model, we also grateful to the State Key Laboratory of Marine Environmental Science (Xiamen University) for sharing the initial field investigation data of COIA.

References

Bao Xianwen, Hou Yijun, Chen Changshen, et al. 2005. Analysis of characteristics and mechanism of current system on the west coast of Guangdong of China in summer. Acta Oceanologica Sinica, 24(4): 1–9

Bauer A, Waniek J J. 2013. Factors affecting chlorophyll *a* concentration in the central Beibu Gulf, South China Sea. Marine Ecology Progress Series, 474: 67–88, doi: 10.3354/meps10075

Cai Lizhe, Fu Sujing, Yang Jie, et al. 2012. Distribution of meiofaunal abundance in relation to environmental factors in Beibu Gulf, South China Sea. Acta Oceanologica Sinica, 31(6): 92–103, doi: 10.1007/s13131-012-0256-2

Chai Fei, Liu Guimei, Xue Huijie, et al. 2009. Seasonal and interannual variability of carbon cycle in South China Sea: A three-dimensional physical-biogeochemical modeling study. Journal of Oceanography, 65(5): 703–720, doi: 10.1007/s10872-009-0061-5

Chen Shengli, Li Yan, Hu Jianyu, et al. 2011. Multiparameter cluster analysis of seasonal variation of water masses in the eastern Beibu Gulf. Journal of Oceanography, 67(6): 709–718, doi: 10.1007/s10872-011-0071-y

Chen Changlin, Li Peiliang, Shi Maochong, et al. 2009a. Numerical

study of the tides and residual currents in the Qiongzhou Strait. Chinese Journal of Oceanology and Limnology, 27(4): 931–942, doi: 10.1007/s00343-009-9193-0

Chen Zhenhua, Qiao Fangli, Xia Changshui, et al. 2015. The numerical investigation of seasonal variation of the cold water mass in the Beibu Gulf and its mechanisms. Acta Oceanologica Sinica, 34(1): 44–54, doi: 10.1007/s13131-015-0595-x

Chen Zuozhi, Qiu Yongsong, Jia Xiaoping, et al. 2008. Using an ecosystem modeling approach to explore possible ecosystem impacts of fishing in the Beibu Gulf, northern South China Sea. Ecosystems, 11(8): 1318–1334, doi: 10.1007/s10021-008-9200-x

Chen Zuozhi, Xu Shannan, Qiu Yongsong, et al. 2009b. Modeling the effects of fishery management and marine protected areas on the Beibu Gulf using spatial ecosystem simulation. Fisheries Research, 100(3): 222–229, doi: 10.1016/j.fishres.2009.08.001

Cheng Gaolei, Gong Wenping, Wang Yaping, et al. 2017. Modeling the circulation and sediment transport in the Beibu Gulf. Acta Oceanologica Sinica, 36(4): 21–30, doi: 10.1007/s13131-017-1012-4

Deetae S, Wisespongpand P. 2001. Sub-thermocline chlorophyll maximum in the South China Sea, area IV: Vietnamese waters. In: Proceedings of the SEAFDEC Seminar on Fishery Resources in the South China Sea, Area IV: Vietnamese Waters. Bangkok, Thailand: Southeast Asian Fisheries Development Center, 251–264

Department of Ocean and Fisheries of Guangxi Zhuang Autonomous Region of China. 2013. 2013 Marine Environment Report of Guangxi Zhuang Autonomous Region (in Chinese). Nanning: Department of Ocean and Fisheries of Guangxi Zhuang Autonomous Region of China

Department of Ocean and Fisheries of Guangxi Zhuang Autonomous Region of China. 2016. 2016 Marine Environment Report of Guangxi Zhuang Autonomous Region (in Chinese). Nanning: Department of Ocean and Fisheries of Guangxi Zhuang Autonomous Region of China

Department of Ocean and Fisheries of Guangxi Zhuang Autonomous Region of China. 2017. 2017 Marine Environment Report of Guangxi Zhuang Autonomous Region (in Chinese). Nanning: Department of Ocean and Fisheries of Guangxi Zhuang Autonomous Region of China

Ding Yang, Chen Changsheng, Beardsley R C, et al. 2013. Observational and model studies of the circulation in the Gulf of Tonkin, South China Sea. Journal of Geophysical Research: Oceans, 118(12): 6495–6510, doi: 10.1002/2013JC009455

Fennel K, Wilkin J, Levin J, et al. 2006. Nitrogen cycling in the Middle Atlantic Bight: Results from a three-dimensional model and implications for the North Atlantic nitrogen budget. Global Biogeochemical Cycles, 20(3): GB3007

Fu Sujing, Cai Lizhe, Yang Jie, et al. 2012. Spatial and seasonal variations of subtidal free-living nematode assemblages in the northern Beibu Gulf, South China Sea. Journal of the Marine Biological Association of the United Kingdom, 92(2): 255–264, doi: 10.1017/S0025315411001056

Gan Jianping, Lu Zhongming, Dai Minhan, et al. 2010. Biological response to intensified upwelling and to a river plume in the northeastern South China Sea: A modeling study. Journal of Geophysical Research: Oceans, 115(C9): C09001

Gao Jingsong, Shi Maochong, Chen Bo, et al. 2014. Responses of the circulation and water mass in the Beibu Gulf to the seasonal forcing regimes. Acta Oceanologica Sinica, 33(7): 1–11, doi: 10.1007/s13131-014-0506-6

Gao Jingsong, Wu Guidan, Ya Hanzheng. 2017. Review of the circulation in the Beibu Gulf, South China Sea. Continental Shelf Research, 138: 106–119, doi: 10.1016/j.csr.2017.02.009

Gao Jingsong, Xue Huijie, Chai Fei, et al. 2013. Modeling the circulation in the gulf of Tonkin, South China Sea. Ocean Dynamics, 63(8): 979–993, doi: 10.1007/s10236-013-0636-y

Guo Mingxian, Chai Fei, Xiu Peng, et al. 2015. Impacts of mesoscale eddies in the South China Sea on biogeochemical cycles. Ocean Dynamics, 65(9–10): 1335–1352, doi: 10.1007/s10236-015-0867-1

Hakuta K, Tabeta S. 2013. Behavioral modeling of Pagrus major in the East Seto Inland Sea. Journal of Marine Science and Technology, 18(4): 535–546, doi: 10.1007/s00773-013-0225-2

Han Baoxin. 2013. Strategic Environmental Assessment of Key Industry Development in the Beibu Gulf Economic Zone (in Chinese). Beijing: China Environmental Press, 8–9

Hu Jianyu, Kawamura H, Tang Danling. 2003. Tidal front around the Hainan Island, northwest of the South China Sea. Journal of Geophysical Research: Oceans, 108(C11): 3342, doi: 10.1029/2003JC001883

Huang Yichen, Li Yan, Shao Hao, et al. 2008. Seasonal variations of sea surface temperature, chlorophyll *a* and turbidity in Beibu Gulf, MODIS imagery study. Journal of Xiamen University (Natural Science) (in Chinese), 47(6): 856–863

Ianson D, Allen S E. 2002. A two-dimensional nitrogen and carbon flux model in a coastal upwelling region. Global Biogeochemical Cycles, 16(1): 11–1

Jiang Rui, Wang Youshao. 2018. Modeling the ecosystem response to summer coastal upwelling in the northern South China Sea. Oceanologia, 60(1): 32–51, doi: 10.1016/j.oceano.2017.05.004

Kano Y, Sato T, Kita J, et al. 2010. Multi-scale modeling of CO_2 dispersion leaked from seafloor off the Japanese coast. Marine Pollution Bulletin, 60(2): 215–224, doi: 10.1016/j.marpolbul.2009.09.024

Kuo N J, Zheng Quanan, Ho C R. 2000. Satellite observation of upwelling along the western coast of the South China Sea. Remote Sensing of Environment, 74(3): 463–470, doi: 10.1016/S0034-4257(00)00138-3

Lai Junxiang, Jiang Fajun, Ke Ke, et al. 2014. Nutrients distribution and trophic status assessment in the northern Beibu Gulf, China. Chinese Journal of Oceanology and Limnology, 32(5): 1128–1144, doi: 10.1007/s00343-014-3199-y

Le T P Q, Billen G, Garnier J, et al. 2010. Nutrient (N, P, Si) transfers in the subtropical Red River system (China and Vietnam): Modelling and budget of nutrient sources and sinks. Journal of Asian Earth Sciences, 37(3): 259–274, doi: 10.1016/j.jseaes.2009.08.010

Li Qian, Wang Yanjun, Dong Yuan, et al. 2015. Modeling long-term change of planktonic ecosystems in the northern South China Sea and the upstream Kuroshio Current. Journal of Geophysical Research: Oceans, 120(6): 3913–3936, doi: 10.1002/2014JC010609

Lin Yuanshao, Cao Wenqing, Yang Shengyun, et al. 2008. Review on environment and bio-resource in Beibu Gulf, with some scientific considerations. In: Hu Jianyu, Yang Shengyun, eds. A Collection of Research Papers on Marine Science in the Beibu Gulf (vol. 1) (in Chinese). Beijing: China Ocean Press, 162–170

Liu Guimei, Chai Fei. 2009. Seasonal and interannual variability of primary and export production in the South China Sea: a three-dimensional physical-biogeochemical model study. ICES Journal of Marine Science, 66(2): 420–431, doi: 10.1093/icesjms/fsn219

Liu K K, Chao S Y, Shaw P T, et al. 2002. Monsoon-forced chlorophyll distribution and primary production in the South China Sea: observations and a numerical study. Deep-Sea Research Part I: Oceanographic Research Papers, 49(8): 1387–1412, doi: 10.1016/S0967-0637(02)00035-3

Liu Zilin, Ning Xiuren, Cai Yuming. 1998. Distribution characteristics of size-fractionated chlorophyll *a* and productivity of phytoplankton in the Beibu Gulf. Haiyang Xuebao (in Chinese), 20(1): 50–57

Ma Lu, Cao Wenqing, Zhang Wenjing, et al. 2014. An ecological study on zooplankton in the northern Beibu Gulf V: the effects of microzooplankton grazing on phytoplankton in summer. Acta Ecologica Sinica (in Chinese), 34(3): 546–554

Mellor G L, Yamada T. 1982. Development of a turbulence closure model for geophysical fluid problems. Reviews of Geophysics, 20(4): 851–875, doi: 10.1029/RG020i004p00851

Minh N N, Patrick M, Florent L, et al. 2014. Tidal characteristics of the Gulf of Tonkin. Continental Shelf Research, 91: 37–56, doi: 10.1016/j.csr.2014.08.003

Mizumukai K, Sato T, Tabeta S, et al. 2008. Numerical studies on ecological effects of artificial mixing of surface and bottom waters in density stratification in semi-enclosed bay and open sea. Ecological Modelling, 214(2–4): 251–270, doi: 10.1016/j.ecolmodel.2008.02.023

Morel A, Berthon J F. 1989. Surface pigments, algal biomass profiles, and potential production of the euphotic layer: Relationships reinvestigated in view of remote-sensing applications. Limnology and Oceanography, 34(8): 1545–1562, doi: 10.4319/lo.1989.34.8.1545

Nakata K. 1993. The canalization of ecosystem model and the illation method of unknown parameter. In: Takahashi M, Nakata K, Parson T R, eds. Advanced Marine Technology Conference (vol. 8) (in Japanese). Tokyo, Japan: Biological Research Press, 99–138

Nakata K, Doi T. 2006. Estimation of primary production in the ocean using a physical-biological coupled ocean carbon cycle model. Environmental Modelling & Software, 21(2): 204–228

Peña M A, Masson D, Callendar W. 2016. Annual plankton dynamics in a coupled physical–biological model of the Strait of Georgia, British Columbia. Progress in Oceanography, 146: 58–74, doi: 10.1016/j.pocean.2016.06.002

Pruszak Z, Van Ninh P, Szmytkiewicz M, et al. 2005. Hydrology and morphology of two river mouth regions (temperate Vistula Delta and subtropical Red River Delta). Oceanologia, 47(3): 365–385

Sato T, Tonoki K, Yoshikawa T, et al. 2006. Numerical and hydraulic simulations of the effect of Density Current Generator in a semi-enclosed tidal bay. Coastal Engineering, 53(1): 49–64, doi: 10.1016/j.coastaleng.2005.08.001

Shi Maochong, Chen Changsheng, Xu Qichun, et al. 2002. The role of Qiongzhou Strait in the seasonal variation of the South China Sea circulation. Journal of Physical Oceanography, 32(1): 103–121, doi: 10.1175/1520-0485(2002)032<0103:TROQSI>2.0.CO;2

Smagorinsky J. 1963. General circulation experiments with the primitive equations: I. The basic experiment. Monthly Weather Review, 91(3): 99–164, doi: 10.1175/1520-0493(1963)091<0099:GCEWTP>2.3.CO;2

Tang Dangling, Kawamura H, Lee M A, et al. 2003. Seasonal and spatial distribution of chlorophyll *a* concentrations and water conditions in the Gulf of Tonkin, South China Sea. Remote Sensing of Environment, 85(4): 475–483, doi: 10.1016/S0034-4257(03)00049-X

Taylor K E. 2001. Summarizing multiple aspects of model performance in a single diagram. Journal of Geophysical Research: Atmospheres, 106(D7): 7183–7192, doi: 10.1029/2000JD900719

The Marine Environment Committee of Japan. 2003. MEC Ocean Model Operation Manual (in Japanese). Tokyo, Japan: Japan Society of Naval Architecture and Ocean Engineering

Thomas W H, Dodson A N. 1972. On nitrogen deficiency in tropical Pacific Oceanic phytoplankton. II. Photosynthetic and cellular characteristics of a chemostat-grown diatom. Limnology and Oceanography, 17(4): 515–523, doi: 10.4319/lo.1972.17.4.0515

Tian Rucheng, Chen Changsheng, Qi Jianhua, et al. 2015. Model study of nutrient and phytoplankton dynamics in the Gulf of Maine: patterns and drivers for seasonal and interannual variability. ICES Journal of Marine Science, 72(2): 388–402, doi: 10.1093/icesjms/fsu090

van Maren D S, Hoekstra P. 2004. Seasonal variation of hydrodynamics and sediment dynamics in a shallow subtropical estuary: the Ba Lat River, Vietnam. Estuarine, Coastal and Shelf Science, 60(3): 529–540, doi: 10.1016/j.ecss.2004.02.011

Van Thuoc C, Huyen N T M, Thu P T, et al. 2012. Some new data on phytoplankton distribution in the western of Tonkin Gulf. Journal of Marine Science and Technology, 12(2): 32–46

Wang Jia, Hong Huasheng, Jiang Yuwu, et al. 2013a. Summer nitrogenous nutrient transport and its fate in the Taiwan Strait: A coupled physical-biological modeling approach. Journal of Geophysical Research: Oceans, 118(9): 4184–4200, doi: 10.1002/jgrc.20300

Wang Fujing, Lin Yuanshao, Cao Wenqing, et al. 2015. The relationship between nutrients and phytoplankton community structure in northern Beibu Gulf. Journal of Tropical Oceanography (in Chinese), 34(6): 73–85

Wang Jun, Luo Zhibin, Pan Weiran, et al. 2013b. The application of ecosystem dynamic model in Xiamen Bay. Journal of Earth Science and Engineering, 3(4): 263–269

Wang Lina, Pan Weiran, Zhuang Wei, et al. 2018. Analysis of seasonal characteristics of water exchange in Beibu Gulf based on a particle tracking model. Regional Studies in Marine Science, 18: 35–43, doi: 10.1016/j.rsma.2017.12.009

Wang Zhe, Tabeta S. 2017. Numerical simulations of ecosystem change due to discharged water from ocean thermal energy conversion plant. In: OCEANS 2017. Aberdeen, Scotland: IEEE, 1–5

Wu Dexing, Wang Yue, Lin Xiaopei, et al. 2008. On the mechanism of the cyclonic circulation in the Gulf of Tonkin in the summer. Journal of Geophysical Research: Oceans, 113(C09): C09029

Yang Jing, Zhang Renduo, Zhao Zhuangming, et al. 2015. Temporal and spatial distribution characteristics of nutrients in the coastal seawater of Guangxi Beibu Gulf during the past 25 years. Ecology and Environmental Sciences (in Chinese), 24(9): 1493–1498

Yu Zhixing, Kyozuka Y. 2003. A simplified moving boundary treatment in the MEC model. In: The Thirteenth International Offshore and Polar Engineering Conference. Honolulu, HI, USA: International Society of Offshore and Polar Engineers, 310–316

Zheng Baiwen, Cao Wenqing, Lin Yuanshao, et al. 2014. Ecosystem structure and function in northern Beibu Gulf II. Quantitative distribution and dominant species of zooplankton. Haiyang Xuebao (in Chinese), 36(4): 82–90

Zheng Qian, Zhang Ruijie, Wang Yinghui, et al. 2012. Occurrence and distribution of antibiotics in the Beibu Gulf, China: impacts of river discharge and aquaculture activities. Marine Environmental Research, 78: 26–33, doi: 10.1016/j.marenvres.2012.03.007

Zhou Meiyu, Lin Yuanshao, Yang Shengyun, et al. 2011. Composition and ecological distribution of ichthyoplankton in eastern Beibu Gulf. Acta Oceanologica Sinica, 30(1): 94–105, doi: 10.1007/s13131-011-0095-6

Supplementary information:

Table S1. The value and meaning of ecological parameters

The supplementary information is available online at https://doi.org/10.1007/s13131-021-1794-2 and www.aosocean.com. The supplementary information is published as submitted, without typesetting or editing. The responsibility for scientific accuracy and content remains entirely with the authors.